

AD-A090 597

CINCINNATI UNIV OHIO

F/6 11/6

DEVELOPMENT OF A MECHANICALLY ALLOYED ALUMINUM ALLOY FOR 450-65--ETC(U)

JAN 80 D L ERICH

F33615-76-C-5227

UNCLASSIFIED

AFML-TR-79-4210

NI

1 of 1

AD-A090 597

END
DATE
FILMED
41-80
DTIC

② LEVEL II

AFML-TR-79-4210



DEVELOPMENT OF A MECHANICALLY ALLOYED ALUMINUM
ALLOY FOR 450-650°F SERVICE

Inco Research & Development Center, Inc.
Sterling Forest
Suffern, NY 10901

January 1980

DTIC
ELECTE
OCT 20 1980
S B D

TECHNICAL REPORT AFML-TR-79-4210

Report Period July 1978 - August 1979

Approved for public release; distribution unlimited.

AIR FORCE MATERIALS LABORATORY
AIR FORCE WRIGHT AERONAUTICAL LABORATORIES
AIR FORCE SYSTEMS COMMAND
WRIGHT-PATTERSON AIR FORCE BASE, OHIO 45433

80

83

AD A090597

DOC FILE COPY

NOTICE

When Government drawings, specifications, or other data are used for any purpose other than in connection with a definitely related Government procurement operation, the United States Government thereby incurs no responsibility nor any obligation whatsoever; and the fact that the government may have formulated, furnished, or in any way supplied the said drawings, specifications, or other data, is not to be regarded by implication or otherwise as in any manner licensing the holder or any other person or corporation, or conveying any rights or permission to manufacture use, or sell any patented invention that may in any way be related thereto.

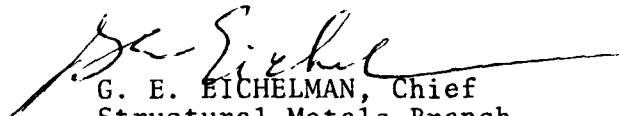
This report has been reviewed by the Office of Public Affairs (ASD/PA) and is releasable to the National Technical Information Service (NTIS). At NTIS, it will be available to the general public, including foreign nations.

This technical report has been reviewed and is approved for publication.



LAWRENCE R. BIDWELL
Program Manager

FOR THE COMMANDER



G. E. EICHELMAN, Chief
Structural Metals Branch
Metals and Ceramics Division

"If your address has changed, if you wish to be removed from our mailing list, or if the addressee is no longer employed by your organization please notify AFWAL/MLLS, W-PAFB, OH 45433 to help us maintain a current mailing list".

Copies of this report should not be returned unless return is required by security considerations, contractual obligations, or notice on a specific document.

SECURITY CLASSIFICATION OF THIS PAGE (When Data Entered)

REPORT DOCUMENTATION PAGE		READ INSTRUCTIONS BEFORE COMPLETING FORM	
1. REPORT NUMBER (18) AFML TR-79-4210	2. GOVT ACCESSION NO. AD-A090597	3. RECIPIENT'S CATALOG NUMBER (9) Final	
4. TITLE (and Subtitle) (6) DEVELOPMENT OF A MECHANICALLY ALLOYED ALUMINUM ALLOY FOR 450-650°F SERVICE.		5. TYPE OF REPORT & PERIOD COVERED Final Report July 1978 - August 1979	
7. AUTHOR(s) (10) D. L. Erich		6. PERFORMING ORG. REPORT NUMBER (30)	
9. PERFORMING ORGANIZATION NAME AND ADDRESS Inco Research & Development Center, Inc. Sterling Forest Suffern, NY 10901		8. CONTRACT OR GRANT NUMBER(s) F33615-76-C-5227	
11. CONTROLLING OFFICE NAME AND ADDRESS Department of Materials Science and Metallurgical Engineering University of Cincinnati, Cinn., OH 45221		10. PROGRAM ELEMENT, PROJECT, TASK AREA & WORK UNIT NUMBERS Project No. 7351 01 75	
14. MONITORING AGENCY NAME & ADDRESS (if different from Controlling Office) Air Force Materials Laboratory (LLS) Air Force Systems Command Wright Patterson Air Force Base, OH 45433		12. REPORT DATE January 1980 13. NUMBER OF PAGES 81	
15. SECURITY CLASS. (of this report) Unclassified		15a. DECLASSIFICATION DOWNGRADING SCHEDULE (12) 94	
16. DISTRIBUTION STATEMENT (of this Report) Approved for public release; distribution unlimited.			
17. DISTRIBUTION STATEMENT (of the abstract entered in Block 20, if different from Report)			
18. SUPPLEMENTARY NOTES Work performed as a sub-contract.			
19. KEY WORDS (Continue on reverse side if necessary and identify by block number) Aluminum Alloys High Temperature Mechanical Alloying Dispersion Strengthening			
20. ABSTRACT (Continue on reverse side if necessary and identify by block number) This investigation was aimed at gaining an understanding of the factors controlling room and elevated temperature strength in aluminum and aluminum alloys prepared by mechanical alloying (M/A). Room temperature strength was found to be controlled by retained cold work, grain size, dispersoid content, precipitation hardening and the presence of low solubility addition elements. Decreasing effectiveness of these factors was found at elevated temperatures			

and, in fact, the solid solution/precipitation hardening elements decreased strength. Stress-rupture and creep properties were defined as a function of stress, time and alloy additions. The most beneficial addition elements were found to be Ti or a combination of Fe+Cr. Stress to produce 0.2% creep strain in 100 hours was estimated to be 22.6 ksi at 450°F and 13.9 ksi at 650°F.

Attempts to improve creep resistance by increasing grain size through variations in hot working were unsuccessful. Creep strength at 450°F was less in the grain coarsened materials than in those with fine grains, and at 650°F was independent of grain size over the limited range evaluated. Thus, subsequent efforts at increasing creep strength will follow the same approach as increasing room and elevated temperature monotonic properties. These efforts will center on improving the quality of solute integration during mechanical alloying and increasing the alloy dispersoid and solute content. Continued attempts at affecting recrystallization to a coarse elongated grain morphology, as achieved in nickel base systems, should be made. Such a structure is expected to increase creep strength at service temperatures greater than 50% of the absolute melting point, 380°F in the case of Al.

FOREWORD

This is the final report under subcontract No. UC-AF-5227, funded by the University of Cincinnati under U.S. Air Force Contract F33615-76-C-5227, Project 7351, with the Structural Metals Branch, Metals and Ceramics Division, Air Force Materials Laboratory. The report covers the period July 1, 1978 to September 30, 1979.

Mr. Robert D. Schelleng served as the Inco Project Coordinator for the program. The experimental work was planned and executed by Dr. Joseph R. Pickens; data interpretation and preparation of the final report was performed by Mr. Donald L. Erich. Mr. Mark E. Rosenblum was the University of Cincinnati Contract Administrator and Dr. Lawrence R. Bidwell was the Air Force Program Manager.

Accession For	
NTIS GRA&I	<input checked="checked" type="checkbox"/>
DTIC TAB	<input type="checkbox"/>
Unannounced	<input type="checkbox"/>
Justification	
by	
Electronic/	
Availability Codes	
Avail and/or	
Dist Special	
A	

TABLE OF CONTENTS

<u>Section</u>		<u>Page</u>
I	INTRODUCTION	1
II	MATERIALS AND PROCEDURES	3
	Unalloyed Compositions	3
	Binary Compositions	3
	Ternary Compositions	4
III	FABRICATION	5
IV	EVALUATION	6
V	RESULTS AND DISCUSSION	7
	Tensile Properties	7
	Unalloyed Material	7
	Binary Alloys	8
	Ternary Alloys	10
	Property Stability	10
	Stress Rupture Properties	10
	Unalloyed Materials	10
	Binary Alloys	10
	Ternary Alloys	11
	Creep Properties	12
	Grain Coarsening Attempts	14
	Unalloyed Al	14
	Al-4Ti	15
	Microstructure	15
	Binary Alloys	15
	Ternary Alloys	18
VI	SUMMARY	19
VII	CONCLUSIONS	21
VIII	RECOMMENDATIONS FOR FURTHER RESEARCH	23
IX	REFERENCES	24

LIST OF TABLES

<u>Table</u>		<u>Page</u>
1	AFML Property Goals and Comparative 2XXX I/M Alloy Performance	25
2	Composition and Dispersoid Content of M/A Unalloyed Al Powders	26
3	Composition and Dispersoid Content of M/A Binary Al Alloy Powders	26
4	Composition and Dispersoid Content of M/A Ternary Al Alloy Powders	26
5	Consolidation and Extrusion Data	27
6	Tensile Properties - Unalloyed Materials	28
7	Room Temperature Base Strength of Unalloyed Materials	29
8	450°F Base Strength of Unalloyed Materials	29
9	Tensile Properties - Binary Alloys	30
10	Base Tensile Strength of Binary Alloys at Various Temperatures	31
11	Contribution of Individual Alloying Elements to R.T. Strength	32
12	Tensile Properties - Ternary Alloys	33
13	Base Tensile Strength of Ternary Alloys at Various Temperatures	34
14	Effect of High Temperature Exposure on R.T. Tensile Properties	35
15	Stress-Rupture Data, Unalloyed Materials	36
16	Stress-Rupture Data, Binary Alloys	37
17	Stress-Rupture Data, Ternary Alloys	38
18	Values of ϵ_I and $\dot{\epsilon}_S$ Obtained from 450°F Creep Tests	39
19	Values of ϵ_I and $\dot{\epsilon}_S$ Obtained from 650°F Creep Tests	40
20	Effect of Thermomechanical Processing Variations on Tensile Properties of Unalloyed Al.	41
21	Effect of Thermomechanical Processing Variations on Stress-Rupture Properties of Unalloyed Al	42
22	Effect of Thermomechanical Processing Variations on the Properties of MA Al-4Ti.	43

LIST OF ILLUSTRATIONS

<u>Figure</u>		<u>Page</u>
1	Room and Elevated Temperature Test Specimen	44
2	Stress-Rupture and Creep Test Specimen	45
3	Schematic Representation of Test Values Obtained from a Creep Curve	46
4	Strength as a Function of Dispersoid Content in Unalloyed Material	47
5	Grain Size as a Function of Volume % Dispersoid	48
6	Effect of Volume % Dispersoid on 450°F Ultimate Tensile Strength - Unalloyed Material	49
7	Effect of Volume % Dispersoid on 550°F and 650°F Ultimate Tensile Strength - Unalloyed Material	50
8	Expected High Temperature (>550°F) Strength Dependence on Dispersoid Content.	51
9	Binary Alloys - 450°F Stress Rupture Properties	52
10	Binary Alloys - 650°F Stress Rupture Properties	53
11	Ternary Alloys - 450°F Stress Rupture Properties	54
12	Ternary Alloys - 650°F Stress Rupture Properties	55
13	Typical Creep Response for MA Al Alloys	56
14	Values of ϵ_I and t_S as a Function of Stress for 450°F Creep Tests	57
15	Values of ϵ_I and t_S as a Function of Stress for 650°F Creep Tests	58
16	Grain Coarsening Resulting from High Temperature, Low Strain Rate Extrusion	59
17	Effect of Coarsened Grains on the 450°F Creep Properties of Al-4Ti	60
18	Effect of Coarsened Grains on the 650°F Creep Properties of Al-4Ti	61
19	Microstructure of M/A Al-3.9Cu	62
20	Microstructure of M/A Al-3.4Mg	63

LIST OF ILLUSTRATIONS (Cont'd)

<u>Figure</u>		<u>Page</u>
21	Microstructure of M/A Al-6.6Zn	64
22	TEMs Comparing Solid Solution Alloys With Unalloyed Material (Longitudinal Sections)	65
23	Microstructure of M/A Al-1.9Cr	66
24	X-ray Elemental Map of Cr and Al in the M/A Al-1.9Cr Material	67
25	Microstructure of M/A Al-1.4Ti	68
26	Microstructure of M/A Al-1.9Mn	69
27	TEMs of Limited Solubility Alloys - M/A Al-1.9Cr, Al-1.7Ti and Al-2Mn (Longitudinal Sections)	70
28	Microstructure of M/A Al-2Co	71
29	Microstructure of M/A Al-1.6Ni	72
30	Microstructure of M/A Al-1.1Fe	73
31	Apparent Evidence of Grain Growth in M/A Al-2Co Alloy	74
32	Grain Coarsening in Unincorporated Ni Particle in M/A Al-1.6Ni Alloy	75
33	No Evidence of Grain Coarsening in M/Al Al-1.1Fe Alloy	76
34	Microstructure of M/A Al-1.8Fe-1.9Ti Alloy	77
35	Microstructure of M/A Al-1.6Fe-1.7Cr Alloy	78
36	Microstructure of M/A Al-1.8Fe-2.4Cr Alloy	79
37	Microstructure of M/A Al-1.8Cr-1.4Ti Alloy	80
38	Microstructure of M/A Al-4Ti Alloy	81

SECTION I

INTRODUCTION

Aluminum alloys with greater strength at elevated temperatures are needed for aircraft applications such as engine compressors and heat exchangers. Current commercial alloys provide high strength at room temperature, but at 450-650°F the strength of these materials decreases rapidly. Consequently, other materials are used for high temperature load carrying applications with a resultant penalty in weight.

The strongest and most commonly used aluminum alloys for high temperature applications are alloys 2219 and 2618. The strengths of these alloys depend on the fineness of the various intermetallic compound particles established during casting, processing and heat treating. The strength of alloy 2219 is derived from its high copper content, 6.3%, which is considerably in excess of the solubility limit. Alloy 2618 contains 1.1% iron and 1% nickel in addition to copper and magnesium. Elevated temperature strength loss in these alloys is due to coarsening of the intermetallic compounds from which strength is derived.

In order to improve the strength of aluminum alloys at high temperatures, more stable strengthening dispersions are needed. Since coarsening of dispersed particles depends on dissolution and diffusion, an obvious choice of dispersoid is aluminum oxide which is essentially insoluble in aluminum. The oxide dispersion strengthened (ODS) materials available heretofore, e.g., SAP, have not fulfilled their promise because of unacceptable combinations of strength and ductility. The high dispersoid contents required for elevated strength resulted in unacceptably low ductility. Consequently, strength had to be sacrificed to gain ductility.

The development of the mechanical alloying process, which provides more uniform dispersions of oxide in aluminum, stimulated renewed interest in ODS aluminum alloys for high temperature service. The present study was initiated to lay the ground work for the development of new high temperature alloys manufactured by this process.

Mechanical alloying is a solid state process whereby elemental or prealloyed powders and oxide particles are combined to produce dispersion strengthened metal powders. During milling the powder particles are repetitively welded and fractured to form composite particles. Organic milling agents can be added to help achieve the required grinding/welding balance. These organic agents also are incorporated into the interior of the powder particles and, on reaction, contribute carbide and oxide particles to the dispersion.

The work conducted in this investigation focused on the effectiveness of two high temperature strengthening mechanisms operative in mechanically alloyed aluminum alloys. First, the relative effectiveness of oxide or carbide dispersoids was studied and, second, the influence of metallic additions (alloying) was assessed. Additionally, the possibility of further strengthening through grain size control via variations in thermomechanical processing was studied. The primary goals established for the work included increased tensile and creep strength at 450 and 650°F with consideration given to high temperature fatigue strength, fracture toughness, fatigue crack growth rate, stress corrosion cracking and post-creep ductility. Table 1* details the tensile and creep goals for the project. Comparative data for several high temperature 2XXX I/M alloys are also included in this table.

* Figures and Tables follow the text.

SECTION II

MATERIALS AND PROCEDURES

Unalloyed Compositions

Six heats of unalloyed MA Al material were selected for evaluation during Phase I of the contract. The objectives of this portion of the study were to determine:

- (a) The effect of variations in the relative amounts of carbide and oxide content on mechanical properties.
- (b) The effect of total dispersoid content on mechanical properties.
- (c) The ability of thermomechanical processing (TMP) variations to affect recrystallization to coarse grains, and its effect on mechanical properties.

Portion (a) of this study was achieved through control of the amounts of oxygen and carbon added during mechanical alloying, Table 2. These constituents are assumed to react to form Al_2O_3 and Al_4C_3 , respectively. Thus, the dispersoid quantity (portion b) is controlled by the total O+C content. The volume percent dispersoid (oxide + carbide) formed is related to the analyzed amount of oxygen and carbon present and the densities of the oxide(1) and carbide(2) phases according to the following expression:

$$\text{Vol.}\% \text{ Dispersoid} = 1.71 \times (\text{wt.}\% \text{ O}) + 3.71 \times (\text{Wt.}\% \text{ C})$$

Portion (c) was investigated through the use of hot rolling and annealing a candidate material. This work is fully discussed in a later portion of the report.

Binary Compositions

Ten binary alloys were evaluated during Task A of Phase II. These alloy additions were selected to exhibit three solubility ranges in the Al base.

(a) Ni, Fe and Co, representing essentially insoluble additions, were added to form stable intermetallic compounds expected to make an additional contribution beyond dispersoid strengthening. Two Fe levels were evaluated to determine the relative effect of alloy content on strength.

(b) Cu, Mn, Cr and Ti, soluble at high temperatures, should contribute to lower temperature strengthening through precipitation hardening at the service temperature.

(c) Zn and Mg, which exhibit extensive solubility at the service temperature, were added to provide solid solution strengthening.

Volume percent dispersoid and carbon/ oxygen volume ratio were maintained at fairly constant levels. The dispersoid content was lower than in Phase I to promote improved ductility. Compositions of these alloys are given in Table 3.

Ternary Compositions

Five additional alloy compositions (Table 4) were selected for study based on the tensile properties of the Task A material. Powder was prepared for evaluation under Task B of Phase II. Four ternaries were made using additions of the lower solubility alloying elements. The solid solution alloys were not considered, as they fell far short of meeting the elevated temperature targets. Because of the promising results obtained with the binary Al-1.7Ti alloy studied in Task A, an Al-4Ti alloy was included for evaluation in Phase II.

SECTION III

FABRICATION

Powder was screened to -30 or -45 mesh, placed in 3.375" O.D., 0.25" thick aluminum cans, and vacuum degassed at 950°F. Degassing times were either 3 or 4 hours and the pump vacuum pressure before consolidation was less than or equal to 200 μ m Hg. Each can was sealed after vacuum degassing and immediately compacted at 950-1000°F at a pressure of 145,000 psi for 20 seconds in a 3.625" diameter chamber. Each compaction was decanned by machining in a lathe.

Extrusion conditions were kept as constant as possible for materials of such diverse compositions. However, some variation in extrusion temperature was found to be necessary to cope with the high flow stresses of these alloys. There are two constraints on the selection of the extrusion temperature: stalling at low temperature due to the increased flow stress, and blistering at high temperature if the stock is heated significantly above the prior powder degassing temperature. The degassing temperature is normally held as low as feasible, since loss of strength can occur with excessively high temperatures. The high flow stress also aggravates the blistering problem because adiabatic heating during extrusion is increased. Considering these constraints, extrusion parameters were selected within the ranges summarized below:

Extrusion Temperature:	650°F to 900°F
Extrusion Ratio:	33.6:1 to 52.6:1 (0.625" rod to 0.5" rod)
Approximate Strain Rate	
Range:	10-30 sec^{-1}

Compaction and extrusion details are contained in Table 5.

SECTION IV

EVALUATION

The tensile properties of all materials were measured in the as-extruded condition at R.T., 450, 550 and 650°F. R.T. tests after 100-hr exposures to either 450 or 650°F were also conducted to determine the structural stability of the M/A materials. Tests were conducted at R.T. according to ASTM standard E-8, and at elevated temperature according to ASTM standard E-21 in Tinius-Olsen Universal Testers. Specimen dimensions are shown in Figure 1.

Creep and stress-rupture tests of as-extruded material were conducted in Riehle static load creep frames according to ASTM standard E-139. Step loaded stress-rupture tests were conducted by applying to each specimen (Figure 2) an initial stress which was increased 2 ksi for 450°F tests and 1 ksi for 650°F tests after 24 hrs if the specimen had not failed. Time spent at the highest applied stress was considered to be the life of the specimen. Creep tests were conducted in a similar manner, except that the time interval between load increments was 100 hrs. Data gathered during these tests included (1) strain on loading to the initial stress, ϵ_0 , (2) the amount of primary creep strain, ϵ_I , defined as the difference between the y-axis intercept of the steady state creep curve and ϵ_0 , and (3) the steady-state creep rate at each load $\dot{\epsilon}_S$. A graphic description of these values is given in Figure 3.

Structural evaluation was done using optical metallography. Standard specimen preparation procedures were used. As-extruded microstructures were recorded at 50 and 200X in the longitudinal and transverse planes. The specimens were etched with either 10% NaOH, Tucker's or Barker's reagent.

A limited number of specimens were examined using transmission electron microscopy. Foils were thinned to perforation in Disa A-2 electropolishing solution, (i.e., 1400 ml reagent alcohol, 240 ml distilled water, 200 ml ethylene glycol monobutyl ether, 156 ml perchloric acid). Structural examination was done in a Phillips EM-300 100 kV electron microscope.

SECTION V

RESULTS AND DISCUSSION

Tensile Properties

Unalloyed Material. Room temperature tensile properties of the unalloyed materials are given in Table 6. Tensile and yield strengths varied depending on dispersoid content as shown in Figure 4. Linear regression analysis of the data yielded correlation coefficients of 0.92 and 0.95 for the tensile and yield strength vs. dispersoid content, respectively. As expected, the tensile strength depends less on dispersoid level than the yield strength. Such behavior is typically exhibited by work hardened materials and results from a decrease in ductility (smaller difference between tensile and yield strength) as strength is increased. Note that extrapolation to 0% dispersoid content results in an estimated tensile strength (subsequently referred to as an alloy "base strength") of 30.5 ksi, a value very close to the tensile strength exhibited by EC Al hardened to the H19 temper (27 ksi)(3). Thus, the base strength of unalloyed M/A Al apparently is due to the retained work hardened state derived from the mechanical alloying process.

Grain size measurements were made from transmission electron microscope (TEM) foils to determine the mechanism by which dispersoid content affects alloy strength. As shown in Figure 5, grain size (as determined by mean intercept length) is independent of dispersoid content for dispersoid levels between 4 and 9 volume percent. Thus, it is the resistance to dislocation flow caused by the presence of dispersoid particles that increases the strength of M/A Al over the (work hardened) base strength. Meiklejohn and Skoda(4) reported a similar relationship between strength and volume fraction precipitate in mercury containing uniformly dispersed iron particles.

Tensile strength at 450°F is also influenced by dispersoid content, although to a lesser extent than room temperature (Figure 6). At 550°F and 650°F, however, changes in dispersoid level between 5 and 10 volume percent exert no influence on strength (Figure 7). Note, however, that the M/A Al strength is far greater than that for non-M/A Al at the same temperature (20 ksi vs. 12.5 ksi, for example, at 650°F)(5). Thus, strength at temperatures $>0.6 T_M$ is enhanced by the presence of dispersoid particles, but there apparently is a maximum concentration above which increases in dispersoid content exert no influence on strength. Ductility is less at these temperatures than at room temperature and this is attributed to high dispersoid content and fine grain size.

The findings of the first portion of this study were used to determine the influence of alloy additions on strength. To do this, a base strength at 0% dispersoid, (i.e., work hardened plus alloy addition increment) was calculated using the relationship developed between dispersoid level and strength. Thus,

$$\text{Alloy Base Strength at R.T.} = \text{UTS (observed)} - 3.41 \times \text{Dispersoid Content}$$

$$\text{Alloy Base Strength at 450°F} = \text{UTS (observed)} - 1.27 \times \text{Dispersoid Content.}$$

Base strengths for the unalloyed materials at R.T. and 450°F are shown in Tables 7 and 8, respectively.

At 550 or 650°F, the dispersoid effect cannot be subtracted because high temperature strength is not affected by changes in dispersoid content at that concentration. The expected strength-dispersoid content relationship is shown in Figure 8; the materials studied so far lie on the horizontal portion of the curve. Thus, the estimated alloy base strength at 550°F or 650°F will include the dispersoid contribution. As a result, estimated 550°F base strengths may be higher than 450°F base strength. Despite this, the values derived are useful to determine the contribution of the alloying elements to strength.

Binary Alloys. In an effort to enhance high temperature ductility, dispersoid level was lowered in these and subsequent heats and attempts were made to achieve strengthening through alloy additions. Mechanical properties of the binary alloys at R.T. are given in Table 9. Note that, except for the Mg and Cu containing alloys, the exhibited strengths are generally less than, and the ductilities greater than those of the unalloyed materials. This is attributed to the decreased dispersoid level of the binary alloys, (3.5-5.5 vs. 5-10 volume % for the unalloyed material). The Cu- and Mg-containing alloys show substantially higher strengths than their unalloyed counterparts, apparently due to the potency of precipitation and/or solid solution hardening. Zinc, an element with high solid solubility, is the least effective strengthener because of its closeness to Al in atomic size (✓7% diametral mismatch compared to ✓11-12% for Cu and Mg)(6). The relative contribution of these alloying elements to strength is shown below:

Mg - 15.9 ksi/atomic %
Cu - 11.4 ksi/atomic %
Zn - 3.1 ksi/atomic %

Note that Mg and Cu, which have limited solubility at R.T., are by far more potent strengtheners than Zn, which has extensive solubility. The relative contribution of each alloying addition to strength is related in part to the amount of lattice strain it produces. Conversely, the solubility is inversely related to the lattice strain. Thus, additions with limited solubility may be expected to make the greatest contribution to alloy strength.

The behavior of the remaining alloying elements is quite different from Cu, Mg and Zn; the contribution to alloy base strength being essentially independent of alloying element (see Table 10). The average contribution of these essentially insoluble and low solubility additions to alloy base strength is 5.5 ksi.

Some slight contributonal differences to strength are seen when the alloy addition contents are considered on a volume basis, (used because of the limited solubility of these elements) Table 11. The most outstanding contribution was made by the low level Fe addition, ~ 16 ksi/vol.% added. Note that the effectiveness of Fe apparently exists only in a limited compositional range. When the volume % addition level is increased from 0.38 to 0.62, the strength change per volume % addition decreases from 16.1 to 7.4 ksi. This behavior implies that a fine dispersion of alloying element was either not established or not maintained during various thermal exposures. This may result from non-optimized mechanical alloying or may be a consequence of using high subsequent processing temperatures. Further comments will be made when the results of the structural analysis are discussed.

The contribution of alloy addition elements to base strength at 450°F is shown in Table 10. The average contribution of the low solubility additions is 2.5 ksi, ranging from a 1.4 ksi base strength loss with Co to a 5 ksi base strength gain with the low-level Fe addition. High-Fe, Mn, Cr and Ti contribute ~ 3 ksi to base strength, while Ni contributes almost nothing. The solid solution elements, Zn, Mg and Cu result in base strength losses at 450°F; the most potent strengtheners at room temperature cause the greatest strength loss at 450°F.

At 550 and 650°F, there is essentially no change in the average alloy base strength, compared to the unalloyed materials (see Table 10). Thus, strength continues to be controlled solely by grain size and dispersoid content. This behavior is also attributed to the lack of a fine dispersion of alloying elements.

Ternary Alloys. The mechanical properties obtained in the ternary alloys are shown in Table 12. A very limited range of strength was obtained; the low UTS value being 53.7 ksi and the high value 55.6 ksi. Alloy base strengths are shown in Table 13. In this case the average increase in base tensile strength is 8 ksi, somewhat lower than might have been expected from extrapolation of the binary alloy data. Study of the bar microstructures, to be discussed later, shows chunks of unalloyed material. Thus, the increase in bulk additions may not reflect accurately the amount of material added as effective, fine dispersoid.

The elevated temperature properties for the ternary alloys are also listed in Tables 12 and 13. Contrary to the behavior exhibited by the binary alloys, strengths higher than the unalloyed materials are observed at every temperature for the ternaries. For example, at 450°F a 6 ksi strength increase is seen in the ternaries, compared to 2.5 ksi in the binaries. Also, nearly 4 ksi strength increases are seen at 550 and 650°F for the ternaries, compared to no increase for the binaries. This behavior may indicate an increasing effectiveness of higher alloy addition levels to improve 550 and 650°F strength.

Property Stability

The effect of 100-hour exposures to 450 or 650°F on the room temperature tensile properties of all materials evaluated in this study is shown in Table 14. Essentially no change in any of the mechanical properties was noted. This behavior indicates resistance to grain or dispersoid particle coarsening and is consistent with other reported findings(7).

Stress Rupture Properties

Unalloyed Materials. All of the unalloyed materials except one failed outside the test section when stress-rupture tested at 450 or 650°F, Table 15. The one material which failed in the test section (83071) contained the lowest dispersoid level, further indicating the need for decreased dispersoid content in the subsequent portions of this work. Some indication of the capabilities of M/A materials to withstand stress at elevated temperature can be obtained from 83071. This material exhibited approximately a 24 hr life at 450°F under a load of 22 ksi; at 650°F, stresses of 16 and 17 ksi caused failure in approximately 1 hour. Note that both these specimens had previously endured at least 24 hours at a 1 ksi lower stress.

Binary Alloys. The 450°F stress rupture properties of the binary alloys are shown in Figure 9. These materials seem to fall into three distinct strength groups: low

strength, exhibited by the materials alloyed with highly soluble elements, Mg, Zn or Cu; intermediate strength, alloys containing Cr, Ni, Fe, Co and Mn and approximating the stress-rupture strength of the unalloyed sample; high strength, showing stress bearing capability in the 26-28 ksi range. Only the Ti-containing alloy had this capability.

At 650°F, three strength groups are again defined (Figure 10). The alloys containing the soluble elements continue to be the weakest, while the strongest materials now include the Ni and low-Fe containing alloys, in addition to the Al-1.65Ti material. The remaining alloys contain Co, Cr, Mn and high Fe and again approximate the properties of the unalloyed composition.

The data obtained from the 450 and 650°F stress-rupture tests (summarized in Table 16) again demonstrate the poor strength of the solid solution strengthened alloys, compared to the strength of the low solubility element containing alloys. Consequently, solid solution alloying elements were not considered in the final portion of this work. Ni, Ti and low Fe additions are seen to exert a beneficial effect on stress-rupture properties, while Co, Cr, Mn and high-Fe have little effect. Because Ni and Co were found to decrease high temperature tensile strength and Mn exhibited marginal 450°F stress-rupture strength, only combined alloy additions of Fe and Ti, Fe and Cr, and Ti and Cr, plus a higher Ti content binary alloy, were evaluated in the final phase of this contract.

Ternary Alloys. The stress-rupture response of the ternary alloys at 450°F is shown in Figure 11. A singular response is exhibited by these materials, regardless of alloy addition. Linear regression analysis of the log stress vs. log life data permits determination of the stress-life relationship. This was found to be:

$$\sigma(\text{ksi}) = 29.5 \cdot t^{-0.033}$$

where $\sigma(\text{ksi})$ = applied stress in ksi, and
t = life in hours

The correlation coefficient for this expression is 0.88.

The 650°F ternary alloy stress-rupture response is shown in Figure 12. As in the binary alloys, non-singular stress-life relationships are exhibited which are in some manner dependent upon the alloying elements. The Fe-Cr and Ti containing alloys are clearly superior to the Fe-Ti and Cr-Ti alloys. The former materials possess both greater strength and a less steep log stress, log life slope than the latter materials (i.e., the life of the former alloys is

less sensitive to changes in stress). This is an excellent combination of characteristics, permitting operation at higher stresses and greater increases in life with relatively smaller load reductions than the Fe-Ti and Cr-Ti alloys. The 450°F and 650°F stress-rupture data for the ternary alloys are summarized in Table 17.

Creep Properties

The ternary alloys were the only ones for which creep behavior was evaluated. Because of the limited number of samples available, these alloys were treated as a single material whenever property similarities appeared. The manner in which the data were interpreted is explained with reference to Figure 3. The creep curves were broken into two plastic strain components: (1) an indication of the amount of strain during primary (stage I) creep, ϵ_I , given by the difference between the extrapolated intercept of the steady-state portion of the creep curve and ϵ_0 , the strain on loading assumed to be all elastic; (2) strain during steady-state creep, $\dot{\epsilon}_s \cdot t$, where $\dot{\epsilon}_s$ is the steady-state creep rate and t is the time length of the test. The initial strain on loading (ϵ_0) was ignored since loads selected for creep testing were well below the 0.2% offset yield stress and examination of the load-deflection curves indicated that the initial deformation is essentially all elastic. The test parameters ϵ_I and $\dot{\epsilon}_s$ were determined for each test and plotted as a function of test stress. In most cases, more than one value of $\dot{\epsilon}_s$ was obtained by step loading the specimens to a higher stress after they had run 100 hours at a given load. This technique did not provide any additional values of ϵ_I , this was limited to the value determined from the first applied stress. The creep response of the Al-1.65Fe-1.68Cr alloy, in this case tested at 650°F, is typical of the behavior of the alloys studied in this contract and is shown in Figure 13.

The values of ϵ_I and $\dot{\epsilon}_s$ obtained from the tests conducted at 450°F are given in Table 18 and plotted against stress in Figure 14. Examination of Figure 14(b) shows that steady-state creep rate increases rapidly with stress except for the Al-1.65Fe-1.68Cr alloy. This material showed an abnormally low steady-state creep rate dependence on stress which, as will be shown in the 650°F test results, was not reproducible. As a result, the data obtained from this test specimen were not included in the interpretation of creep response to stress. Ignoring those data points, the following linear functional relationships were obtained:

$$\epsilon_I = 4 \times 10^{-4} \sigma(\text{ksi}) - 7.9 \times 10^{-3} \quad ; r=0.57$$

$$\dot{\epsilon}_s(\text{hr}^{-1}) = 5.7 \times 10^{-6} \sigma(\text{ksi}) - 1.2 \times 10^{-4} \quad ; r=0.87$$

Note that some of the correlation coefficients in this and the subsequent analysis are somewhat low. Although these indicate poor linear correlation, they do support the existence of trends. Due to the lack of adequate data on each alloy to perform individual analyses, estimates must be made using this approach. The total creep strain as a function of stress and the time is given by:

$$\epsilon_T = \epsilon_I + \dot{\epsilon}_S \cdot t$$

where ϵ_T is the total creep strain, and ϵ_I and $\dot{\epsilon}_S$ are functions of stress. Rearrangement of the equations and substitution of 0.002 for ϵ_T and 100 hours for t permits estimation of the stress which will result in 0.2% creep strain in 100 hours. The value obtained for these materials at 450°F is 22.6 ksi.

A similar treatment was performed for the creep data generated at 650°F. The values of ϵ_I and $\dot{\epsilon}_S$ are presented in Table 19 and plotted against stress in Figure 15. Steady-state creep rate for one of the Al-1.65Fe-1.68Cr alloys again shows an abnormally low dependence on stress. However, a second specimen behaved in a manner similar to the remaining test specimens. As a result, the first set of data were not used for the subsequent analysis. Another specimen exhibiting unusual behavior was the Al-1.8Cr-1.8Ti alloy. When loaded to 11 ksi, this specimen showed an extremely high value for steady-state creep rate while, when loaded to 12 ksi, the rate dropped to a more representative value. Consequently, the first creep rate datum of that test was also ignored. Estimation of the expressions for ϵ_I and $\dot{\epsilon}_S$ resulted in the following:

$$\epsilon_I = 2.35 \times 10^{-4} \sigma(\text{ksi}) - 2 \times 10^{-3} \quad ; r=0.44$$

$$\dot{\epsilon}_S(\text{hr}^{-1}) = 2.6 \times 10^{-6} \sigma(\text{ksi}) - 2.9 \times 10^{-5} \quad ; r=0.76$$

Use of these expressions results in a calculated value of 13.9 ksi for 0.2% creep strain in 100 hours at 650°F.

Although this stress is below the target value of 18 ksi for a 100-hour test, the benefit of dispersion strengthening becomes apparent when the stress for 0.2% strain in 1000 hours is calculated. This value is estimated to be 11.6 ksi and exceeds the target value of 10 ksi by a comfortable margin. This low dependence of stress on time is typical of dispersion strengthened materials and indicates a unique advantage over conventionally made alloys. The advantage is a direct result of the presence of phases essentially inert, compared to the intermetallic compounds usually used for strengthening in conventional I/M alloys.

Grain Coarsening Attempts

Unalloyed Al. Grain coarsening through modifications in thermomechanical processing (TMP) of MA Al (83060) involved hot rolling and annealing treatments. The 0.625" dia. extruded bar was hot rolled to 0.312" dia. (75% reduction of area) at either 750, 850 or 950°F. Room temperature tensile properties were determined from the as-rolled pieces. The remaining bar was then annealed at 950°F for 1 hour. Mechanical property evaluation involved static tensile testing at room and elevated temperatures (450, 550 and 650°F) for material rolled at 750 or 950°F and annealed. Bar rolled at 850°F and annealed at 1050°F was stress-rupture tested at 450 and 650°F.

The effect of hot rolling-annealing combinations on the tensile properties of unalloyed MA Al (83060) is shown in Table 20. The most significant effect on tensile properties is in the greatly increased ductility at all test temperatures. A factor of two improvement in tensile elongation is realized at room temperature (6% to 512% after TMP) and 450°F (4.5% to 9% after TMP), with even greater improvements seen at 550 and 650°F. Significant improvements in % RA were also obtained, except at room temperature, where some decrease was generally observed. However, even though less than before TMP, room temperature RA is still >40%. No improvement in elevated temperature tensile strength results from this TMP operation. However, room temperature yield strength decreased, particularly after the 1050°F/1 hour anneal.

Stress-rupture properties before and after modified TMP are shown in Table 21. Although substantial strength increases at 450°F are realized with the TMP material, this is probably a result of the improved ductility rather than a real improvement in strength. No strength advantage of TMP appears in the tests conducted at 650°F.

Quantitative metallography was performed on the standard processed bar and on bar rolled at 950°F and annealed at 1050°F. The results of this analysis showed that only slight grain coarsening was achieved by the TMP variation. The standard material exhibited a mean grain size of 0.19 μm with a standard deviation of 0.03 μm , while the mean grain size and standard deviation of the TMP material was 0.24 μm and 0.08 μm , respectively. Thus, it is concluded that this TMP attempt was generally unsuccessful at effecting grain growth.

Al-4Ti. The second attempt at grain coarsening was made on material from powder lot 83089 (Al-4Ti). This processing variation included degassing, compaction and extrusion to 0.625" dia at 1050°F. Further, the strain rate during extrusion of this bar was $\dot{\epsilon}$ 1.9 sec⁻¹, compared to the typical value of >10 sec⁻¹ used for the other bar. Because of material restrictions, testing was limited to tensile tests at R.T., 450 and 650°F and creep testing at 450 and 650°F.

Increased grain size was achieved using this technique as shown in Figure 16. Bar extruded at 800°F shows fine, irregularly shaped grains and a high concentration of grey and black regions. After slower strain rate extrusion at 1050°F these features are not observed and coarse, equiaxed grains are present. Tensile properties, shown in Table 22, reflect the increased grain size. Substantial room temperature strength loss is observed with less striking losses at 450°F and 650°F. The room temperature UTS dropped from 55.6 ksi to 37.7 ksi, as a result of the higher temperature, lower strain rate extrusion. At 650°F the drop was from 27 to 23.5 ksi.

The effect of increased grain size on creep properties is shown in Figures 17 and 18. At 450°F (Figure 17) the grain coarsened material exhibited inferior primary creep resistance and greater steady-state creep rate. The greatest differences between primary creep strains from the two processing conditions was noted at low stress (e.g., 17 ksi), whereas at stresses $\dot{\epsilon}$ 23 ksi, very little difference in response was noted. Steady-state creep rate suffered doubly as a result of TMP; both the intercept and slope of the log $\dot{\epsilon}_s$ vs. log σ curve are greater for the TMP variant than for the lower temperature, higher strain rate extruded material. At 650°F (Figure 18), the high temperature, low strain rate processing makes no difference to steady-state creep rate and only slightly affects the primary creep strain response. Thus, grain coarsening of these materials results in decreased creep resistance at temperatures less than 650°F and shows no benefit at 650°F. The conclusion to be drawn from this work is that creep resistance at temperatures around 450°F apparently will be increased by processing modifications aimed at increasing static properties. Thus, improvements will likely be obtained from increased dispersoid content, decreased grain size and increased alloy additions.

Microstructure

Binary Alloys. Optical micrographs of longitudinal and transverse sections of the alloys made with the most soluble alloying elements, Cu, Mg and Zn, are shown in

Figures 19-21. The Al-3.9Cu alloy, (Figure 19) exhibiting the least solid solubility of these alloys, shows a uniform dispersion of an equiaxed second phase and essentially no strung-out particles. The second phase particles, which have a maximum dimension of about 5-10 μm , are believed to be coarse θ , Al_2Cu , which formed during the 700°F heat-up for extrusion. The lack of stringers in the bar is an indication of the ease with which this mixture can be mechanically alloyed.

The Al-3.4Mg alloy (Figure 20) shows a clean structure with few stringers and no evidence of precipitates. The lack of precipitates is as expected, since this composition does not exceed the solid solubility of Mg in Al until temperatures lower than about 200°F are reached.

A fine, uniform dispersion of an unidentified second phase and occasional elongated, white regions believed to be unincorporated zinc, are seen in the Al-6.6Zn micrographs (Figure 21). Transmission electron micrographs of the Cu, Mg and Zn containing alloys are shown in Figure 22. All three materials show similar grain sizes, approximately 0.18 μm determined by the linear intercept technique. The Cu containing alloy appears to contain a dispersion which may be fine Al_2Cu , while the very fine phase visible in the Al-Mg alloy is believed to be the oxide and carbide dispersoid particles. For comparison, a TEM of unalloyed material is also shown in Figure 22.

The microstructures of the alloys showing limited solubility (solid solubility at the melting point less than 2 weight %) are shown in Figures 23, 25 and 26. The Al-1.9Cr alloy (Figure 23) shows the presence of coarse grey particles. Electron microprobe analysis (EMPA) of these particles identified two distinct compositions: elemental Cr, and an intermetallic compound with Al and Cr ratios nearly equal to that of the equilibrium compound, Al_7Cr . An x-ray map depicting both phases in the Al-rich matrix is shown in Figure 24. The presence of elemental Cr is an obvious indication of incomplete powder processing. The intermetallic compound is presumed to have formed by interdiffusion of Al and Cr rather than by particle coarsening. Selective formation of the intermetallic compound is assumed to have resulted from variations in the Cr to Al bonding (wetting) during processing. Note that the elemental Cr shows a distinct boundary with the Al, thus preventing atomic transport.

The Al-1.4Ti alloy is shown in Figure 25. The presence of numerous elongated stringers in the longitudinal section and short, elongated regions in the transverse section indicates advanced, but incomplete incorporation of

the Ti into the Al powder during mechanical alloying. The severe attack of the stringers when etched in a hydrofluoric acid containing solution verified that they are essentially unalloyed Ti.

The Al-1.9Mn alloy (Figure 26) is similar to the Al-Cr material. Many apparently unincorporated particles are observed and, on examination in the microprobe, these were found to be elemental Mn or coarse Al_6Mn particles.

TEM's of the above three alloys, Figure 27, again show similarities in grain size, independent of alloy additions. No evidence of very fine intermetallic dispersoids is present, reflecting poor incorporation of the alloying elements during mechanical alloying.

Microstructures of the alloys made with essentially insoluble additions are shown in Figures 28-30. Micrographs of the Al-2Co alloy (Figure 28) show a generally uniform distribution of fine ($<1\text{ }\mu\text{m}$) second phase particles and an occasional larger, 5-25 μm , grey particles. Except for the occasional larger particle, the Al-Co material appears to be well processed.

The Al-1.6Ni structure is shown in Figure 29. Large white patches, believed to be unalloyed Ni, appear in both the longitudinal and transverse sections. The additional particles visible may be either added Ni or Fe contamination picked-up during processing.

The microstructure of the Al-1.1Fe alloy is shown in Figure 30. Only an occasional white streak is evident, implying relatively easy incorporation of the Fe addition into the Al matrix. A very fine, uniformly distributed phase, presumed to be the Al_3Fe intermetallic compound, is also present.

TEM's of the above three materials are shown in Figures 31-33. In general, the grain size of these alloys are nearly equal but occasional evidence of grain coarsening was observed. Figures 31a and b (Al-Co alloy) show areas which are similar microstructurally, except for the presence of large grains, thus implying the ability of the grains to coarsen under certain conditions. Figures 32a and b, the Al-Ni alloy, show two distinct microstructural types; a fine grain region containing a high concentration of particles, and a coarse grain region containing a relatively low concentration of well defined, spherical particles. Figure 32c shows the interface between the fine and coarse grain regions, believed to mark the location of the unalloyed

Ni. Thus, the presence of coarse grains in this case results from the absence of grain size controlling dispersoid particles. No regions containing coarse grains were seen in the Al-Fe alloy, Figure 33.

Ternary Alloys. The microstructures of the ternary alloys are shown in Figures 34-38. In general, the appearance of these materials could have been predicted from the binary structures. The Al-1.8Fe-1.9Ti alloy structure (Figure 34) consists of regions of unincorporated Ti (grey particles) and small regions rich in Fe (white streaks). The two Al-Fe-Cr alloys, Figures 35-36, similarly show white, blocky Cr particles and white Fe streaks. The Al-1.8Cr-1.8Ti structure, Figure 37, shows the typical, strung-out, grey Ti particles and blocky, white Cr particles. The structure of the Al-4Ti alloy, shown in Figure 38, is quite similar to the lower alloyed, 1.4Ti composition.

SECTION VI

SUMMARY

This investigation was aimed at gaining an understanding of the factors controlling room and elevated temperature strength in aluminum alloys prepared by mechanical alloying (M/A). Five factors were found to contribute to strength at room temperature:

- (1) Retained cold work - caused by severely cold working the powder during mechanical alloying and retarding the recovery process by introducing dispersoid. This results in an Al base strength equal to that of EC Al hardened to the H19 temper.
- (2) Fine grain size - stabilized by the presence of oxide and carbide particles which, if present in sufficient quantity, render the material virtually immune to grain growth.
- (3) Oxygen plus carbon content - determines the quantity of dispersoid which will form by reaction to Al_2O_3 and Al_4C_3 , respectively. In addition to stabilizing the microstructure, dispersoid content apparently contributes to strength by impeding dislocation movement.
- (4) Solid solution/precipitation hardening - Cu and Mg additions were found to exert a profound influence on strength, presumably through precipitation and solid solution hardening. Unfortunately, these elements and Zn severely decreased elevated temperature properties.
- (5) Low solubility addition elements - had limited strengthening effectiveness which was essentially independent of the element selected and was not linearly related to alloy content. These responses are attributed to incomplete micro-incorporation of the alloying elements during processing. The presence of coarse, unalloyed particles, or intermetallic compounds formed by interdiffusion, is evidence that the full strengthening contribution of the additions never occurred. Thus, estimations of strengthening contribution per alloying element are conservative.

Tensile properties at 450°F also depended on dispersoid and low solubility element content, but to a lesser extent than at room temperature. At 550 and 650°F, tensile properties continued to be slightly influenced by

low solubility element content but they were independent of changes in dispersoid content. This is assumed to reflect an overwhelming influence of the fine grain size on controlling strength compared to the interference of dislocation motion by dispersoid particles. The stabilizing effect of the dispersoid particles on grain size is further demonstrated by the absence of room temperature strength loss following 100-hour exposures at temperatures as high as 650°F.

Creep and stress-rupture properties were also influenced by alloy additions; Mg, Cu and Zn adversely affected properties, while the low solubility additions did not harm, and in some cases improved, strengths. The alloy additions most beneficial to stress rupture properties were Ti or a combination of Fe and Cr. Combinations of Cr + Ti or Fe + Ti did not improve properties beyond those exhibited by the unalloyed materials.

Creep response, evaluated only for the ternary alloys, appeared to be independent of alloying element addition. Assuming this independence permitted definition of total creep strain as a function of stress and time. Estimates of the stresses required to produce 0.2% creep strain in 100 hours are 22.6 ksi at 450°F and 13.9 ksi at 650°F, somewhat below the target values of 36 and 18 ksi, respectively. However, extrapolation of the data to 1000 hours resulted in an estimated 11.6 ksi stress required to cause 0.2% creep deformation at 650°F. This value exceeds the target stress of 10 ksi by a comfortable margin and indicates a unique advantage of mechanical alloying over conventional processing. The advantage is the ability to introduce an essentially inert, fine dispersion uniformly distributed throughout the matrix. The dispersion acts as an effective barrier to dislocation motion at high temperature.

Material variations needed to increase strength at the lower temperature regime were indicated by the negative response of grain coarsening studies. Both tensile strength (at R.T. or 450°F) and creep resistance decreased as grain size increased, indicating a similar influence of grain size on both these properties. Additionally, coarsening of the grains had no effect on 650°F creep properties. Thus, efforts to bring about the desired increase in tensile strength, namely increasing alloy content and dispersoid level, are not expected to exert a deleterious effect on creep properties, even though they would further stabilize the alloy's fine grain size.

SECTION VII

CONCLUSIONS

1. Room temperature tensile properties in mechanically alloyed materials are controlled by retained cold work, grain size, dispersoid content, solid solution and precipitation hardening and by the presence of low solubility addition elements.

2. Solid solution and precipitation hardened alloys possess lower strength at elevated temperature ($\geq 450^{\circ}\text{F}$) than unalloyed materials of comparable dispersoid level.

3. 450°F tensile properties in unalloyed and low solubility addition element containing alloys are controlled by dispersoid content, but to a lesser extent than at room temperature.

4. 450°F tensile properties increase slightly with increasing quantity of low solubility addition element.

5. 550°F and 650°F tensile properties are independent of changes in dispersoid content.

6. 550°F and 650°F tensile properties increase slightly with sufficiently high quantities of low solubility alloying elements.

7. Room temperature tensile properties are not altered by 100-hour exposures at 450 or 650°F .

8. 450°F and 650°F stress-rupture properties are adversely affected by additions of Mg, Cu or Zn (i.e., solid solution/precipitation hardened alloys).

9. 450°F and 650°F stress-rupture properties are generally improved by additions of low solubility elements compared to unalloyed material.

10. 650°F stress-rupture properties are improved most by additions of Ti or Fe + Cr.

11. Creep response (not evaluated for solid solution/precipitation hardened materials) is independent of alloying element additions.

12. The stresses estimated to produce 0.2% creep strain in 100 hours at 450°F and 650°F are 22.6 and 13.9 ksi, respectively.

13. Mechanically alloyed aluminum alloys exceed the stress goal for 0.2% creep strain in 1000 hours at 650°F, (11.6 ksi estimated vs. 10 ksi target).

14. Recrystallization to coarse grain size was not produced by thermomechanical processing variations.

SECTION VIII

RECOMMENDATIONS FOR FURTHER RESEARCH

Further studies aimed at developing a high strength Al alloy made by mechanical alloying (M/A) should concentrate on the following areas:

(a) Improved alloying element incorporation. Some of the alloys prepared under this contract showed evidence of non-optimum attritor processing. This resulted from differences in the response of the wide variety of compositions studied to the "standard" attritor operating conditions selected. Improved processing would be expected to lead to improved mechanical properties. The use of prealloyed Al powders may be helpful in this respect.

(b) Optimized alloy content and composition. The response of mechanical properties to increasing intermetallic compound content was not satisfactorily defined because of inefficiencies in alloying element incorporation. Further, the optimum mix of intermetallic and oxide and carbide dispersoids remains to be defined. Determination of the effects of these variables on tensile and creep properties would allow definition of an optimized alloy composition for high temperature use.

(c) Clarification of grain size effects. Anomalous results concerning the benefit of coarsened grains on creep properties were obtained in this study. Improved creep properties expected to accompany grain coarsening were not observed. Further studies to define the trade-off between softening associated with stress relief and creep resistance associated with greatly increased grain size is required. Processing modifications which will produce coarse, elongated grain structures, analogous to those which result in improved creep properties in MA Ni alloys, remain to be defined.

(d) Structural studies. Information regarding the shape, size, quantity, distribution and stability of intermetallic, oxide and carbide phases is required. By systematically varying the relative amounts of these phases, their effect on mechanical properties could be determined.

Concerted research in these four areas would be expected to lead to compositional and structural definition of an MA alloy or alloys ideally suited for high temperature application.

SECTION IX

REFERENCES

1. N. Hansen, Trans. TMS AIME, 245, 1969, p. 1350ff.
2. Powder Diffraction File, Inorganic Volume No. PD1S-51RB; published by the Joint Committee on Powder Diffraction Standards, Swarthmore, PA, 1974.
3. Aluminum, 1, 312 (1967), American Society for Metals, Metals Park, OH 44073.
4. W. H. Meiklejohn and R. E. Skoda, Acta. Met., 8, pp. 733-780 (1960).
5. Metals Handbook, 8th Ed., 1, 936 (1961), American Society for Metals, Metals Park, OH 44073.
6. Elements of X-ray Diffraction, 484, (1956), Addison-Wesley Publishing Co., Inc., Reading, MA.
7. P. S. Gilman, Ph.D. Dissertation, Stanford University, Stanford, CA (1979).

Table 1*. AFML Property Goals and Comparative 2XXX I/M Alloy Performance.

AFML Goal 2219-T851 2024-T851 2618-T851

Tensile Properties

75°F

Yield Strength, ksi	58	50	65	54
Tensile Strength, ksi	62	66	70	64
Elongation, %	5.0	12.0	8.0	10.0

450°F

Yield Strength, ksi	50	27	18	26
Tensile Strength, ksi	55	32	25	28
0.2% Creep, 100 hrs, ksi	36	12	12	-
0.2% Creep, 1000 hrs, ksi	32	-	-	-

650°F

Yield Strength, ksi	35	7.9	5.3	4.8
Tensile Strength, ksi	40	9.4	7.3	6.5
0.2% Creep, 100 hrs, ksi	18	4.9	-	-
0.2% Creep, 1000 hrs, ksi	10	-	-	-

*Portions of this table were extracted from Elevated Temperature Al Alloy Development, Alcoa Technical Report, for the period 1978 March 29 to 1979 March 28.

Table 2. Composition and Dispersoid Content of M/A Unalloyed Al Powders.

Alloy Identification	O	C	Fe	Dispersoid (Vol.%) [*]	Carbide (Oxide) by Vol.
83060	1.36	1.25	.11	6.95	1.99
83062	2.39	1.08	.049	8.10	.98
83071	1.75	.53	.13	4.96	.66
83072	1.29	1.78	.21	8.80	3.00
83083	1.47	1.97	.14	9.82	2.90
83088	1.27	1.39	.044	7.33	2.37

$$*\text{Vol.}\% \text{ Dispersoid} = 1.71 \times (\text{wt.}\% \text{ O}) + 3.71 \times (\text{wt.}\% \text{ C}).$$

Table 3. Composition and Dispersoid Content of M/A Binary Al Alloy Powders.

Alloy Identification	Alloy Addition	O	C	v/o Dispersoid [*]
83074	Fe 1.79	1.41	.49	4.23
83076	Co 1.98	1.41	.51	4.30
83079	Ti 1.65	1.37	.54	4.34
83081	Fe 1.09	1.95	.60	5.56
83085	Mg 3.4	1.33	.59	4.46
83086	Mn 1.92	1.53	.53	4.58
83087	Zn 6.6	1.86	.51	5.07
83696	Ni 1.60	1.73	.36	4.29
83697	Cr 1.87	1.26	.39	3.60
83698	Cu 3.9	1.43	.46	4.15

$$*\text{Vol.}\% \text{ Dispersoid} = 1.71 \times (\text{wt.}\% \text{ O}) + 3.71 \times (\text{wt.}\% \text{ C}).$$

Table 4. Composition and Dispersoid Content of M/A Ternary Al Powders.

Alloy Identification	Alloy Addition	O	C	v/o Dispersoid [*]
83700	1.75Fe + 1.95Ti	1.46	0.45	4.17
83702	1.65Fe + 1.68Cr	1.70	0.54	4.91
83703	1.77Fe + 2.35Cr	1.56	0.48	4.45
83704	1.82Cr + 1.39Ti	1.60	0.53	4.70
83089	4.0 Ti	2.11	0.47	5.35

$$*\text{Vol.}\% \text{ Dispersoid} = 1.71 \times (\text{wt.}\% \text{ O}) + 3.71 \times (\text{wt.}\% \text{ C}).$$

Table 5. Consolidation and Extrusion Data

Alloy Identification	Degas/Compaction Temp (°F)	Degas Time (hrs)	Vacuum Pressure Before Compaction		Extrusion Preheat Temp. (°F)	Billet Preheat Time (hrs)	Throttle Setting (%)	Extrusion Ratio	Comments
			(um)						
Unalloyed									
83062	950	3	200		900	3-3/4	50	52.6	Some surface cracking
83071	950	3	200		900	3-3/4	15	52.6	Minor blistering
83072	950	3	200		900	3-3/4	50	33.6	Good extrusion
83073	950	3	140		850	3-3/4	35	33.6	Minor blistering
83088	950	3	80		850	3-3/4	35	33.6	Minor blistering
83060	1050	3	10		650	2		33.6	
Binary Alloys									
83074-Fe	950	3	50		850	3-3/4	30	33.6	Good extrusion
83076-Co	950	3	30		707	4-1/2	30	33.6	Good extrusion
83079-Ti	950	3	45		750	2	30	33.6	Some surface cracking
83081-Fe	950	3	50		700	4-1/2	30	33.6	Good extrusion
83085-Mg	950	3	60		800	2-1/2	30	33.6	Good extrusion
83086-Mn	950	3	50		750	2	30	33.6	Some surface cracking
83087-Zn	950	3	180		750	2	30	33.6	Good extrusion
83696-Mi	1000	3	50		700	2	30	33.6	Good extrusion
83697-Cr	1000	3	50		700	2	30	33.6	Good extrusion
83698-Cu	1000	3	30		700	2	30	33.6	Good extrusion
Ternary Alloys									
83700-Fe-Ti	950	4	80		800	3	30	33.6	Good extrusion
83702-Fe-Ti	950	4	50		800	3	30	33.6	Good extrusion
83703-Fe-Ti	950	4	50		800	3	30	33.6	Good extrusion
83704-Cr-Ti	950	4	80		800	3	30	33.6	Good extrusion
83705-Ti	950	4	110		800	3	30	33.6	Good extrusion

Table 6 . Tensile Properties - Unalloyed Materials

Alloy Identification	v/o Dispersoid*	Carbide* Oxide	70°F				450°F				550°F				650°F			
			UTS (ksi)	YS (ksi)	El. (%)	RA (%)	UTS (ksi)	YS (ksi)	El. (%)	RA (%)	UTS (ksi)	YS (ksi)	El. (%)	RA (%)	UTS (ksi)	YS (ksi)	El. (%)	RA (%)
83060	6.95	1.99	51.8	46.3	6	60	31.6	27.6	4.5	16	26.4	23.7	2	3	19.9	-	1	0
83062	8.10	.98	55.5	50.7	5.5	17.5	31.5	29.1	2	4.5	25.8	25.8	0	0	18.7	-	0	0
83071	4.96	.66	47.7	39.9	12	44	30.4	27.2	3.5	18.5	26.5	23.8	3.5	14	21.6	19.8	2	5.5
83072	8.80	3.00	60.6	55.5	8	32.8	32.6	27.6	2	3.5	26.1	23.3	2	5.5	18.9	18.9	2	1.5
83083	9.82	2.90	64.8	58.3	6.5	34	37.8	31.8	1	0	25.1	24.6	1	0	22.6	22.2	1	0
83088	7.33	2.37	59.5	53.4	9	36	30.6	29.7	1	3	24.3	24.3	1	2	18.7	-	0	0

*Based on volumes.

Table 7. Room Temperature Base Strength of Unalloyed Materials.

<u>Alloy Identification</u>	<u>v/o Dispersoid</u>	<u>UTS (ksi)</u>	<u>σ_0^* (ksi)</u>
83060	6.95	51.8	28.1
83062	8.18	55.5	27.6
83071	4.66	47.7	30.8
83072	8.80	60.6	30.6
83083	9.82	64.8	31.3
83088	7.33	59.5	34.5

mean = 30.5
standard deviation = 2.5

* $\sigma_0 = \text{UTS} - 3.41 \times (\text{v/o dispersoid}) = \text{base strength.}$

where 3.41 is the slope of the UTS vs. v/o dispersoid curve, thus σ_0 is the predicted strength of each heat at 0% dispersoid. Note that the mean 30.5 ksi, is approximately the strength observed in EC Al hardened to the H19 temper.

Table 8. 450°F Base Strength of Unalloyed Materials.

<u>Alloy Identification</u>	<u>v/o Dispersoid</u>	<u>UTS (ksi)</u>	<u>σ_0^* (ksi)</u>
83060	6.95	31.6	22.8
83062	8.18	31.5	21.1
83071	4.96	30.4	24.1
83072	8.80	32.6	21.4
83083	9.82	37.8	25.3
83088	7.33	30.6	21.3

mean = 22.7
standard deviation = 1.7

* $\sigma_0 = \text{UTS} - 1.27 \times (\text{v/o dispersoid}) = 450^\circ\text{F base strength.}$

where 1.27 is the slope of the UTS vs. v/o dispersoid curve.

Table 9 . Tensile Properties - Binary Alloys

Alloy Identification	Comp.	70°F					450°F					550°F					650°F				
		UTS (ksi)	YS (ksi)	El. (%)	RA (%)		UTS (ksi)	YS (ksi)	El. (%)	RA (%)		UTS (ksi)	YS (ksi)	El. (%)	RA (%)		UTS (ksi)	YS (ksi)	El. (%)	RA (%)	
83074	1.79 Fe	49.5	42.2	8	26		31.9	28.5	3.5	14		27.1	24.9	4.5	12.5		21.2	20.2	2	8	
83076	1.98 Co	49.4	42.2	17.5	57.5		26.8	24.1	5	23.5		22.2	20.3	2	14		18.7	18.4	1	4	
83079	1.65 Ti	52.4	45.8	11.5	48		31.3	27.1	10	24		25.8	22.5	10.5	22		22.8	20.3	2.5	14	
83081	1.09 Fe	55.6	48.2	9.5	30.5		34.8	30.0	5.5	15		28.7	25.8	2	5		21.7	-	0.5	0.75	
83085	3.4 Mg	89.0	78.5	6	30		21.7	17.5	51	88		15.2	13.7	18	83		12.5	11.0	16.5	79.5	
83086	1.92 Mn	52.8	44.9	10.5	28.5		32.2	28.1	8	10.5		26.3	23.7	2	6.5		18.3	-	.5	2	
83087	6.6 Zn	56.5	49.6	9	27.5		27.0	22.3	1.5	1		18.1	18.1	0	0		13.1	-	0	0	
83696	1.60 Ni	49.0	41.2	15	47		28.2	25.2	10.5	33.5		22.8	22.3	6	28		19.8	19.5	2.5	2	
83697	1.87 Cr	48.4	42.6	9.5	31		30.6	26.7	8.5	19.6		25.3	22.4	6.5	17.2		20.9	19.5	4	17	
83698	3.9 Cu	63.6	55.3	8.5	17		18.2	17.5	14.5	53.5		15.5	15.2	6	23.5		12.9	12.9	2	3	

Table 10. Base Tensile Strength of Binary Alloys at Various Temperatures.

Alloy Identification	Addition	v/o Dispersoid	R.T		450°F		550°F		650°F	
			UTS (ksi)	σ_0^* (ksi)	UTS (ksi)	σ_0^* (ksi)	UTS (4) (ksi)	σ_0^* (ksi)	UTS (4) (ksi)	σ_0^* (ksi)
83074	Fe	4.23	49.5	35.1	31.9	26.5	27.1		21.2	
83076	Co	4.30	49.4	34.7	26.8	21.3	22.2		18.7	
83079	Ti	4.34	52.4	37.6	31.3	25.8	25.8		22.8	
83081	Fe	5.56	55.6	36.6	34.8	27.7	28.7		21.7	
83085	Mg	4.46	89.0	73.8	21.7	16.0	15.2		12.5	
83086	Mn	4.58	52.8	37.2	32.2	26.4	26.3		18.3	
83087	Zn	5.07	56.5	39.2	27.0	20.6	18.1		13.1	
83696	Ni	4.29	49.0	34.4	28.2	22.8	22.8		19.8	
83697	Cr	3.60	48.4	36.1	30.6	26.0	25.3		20.9	
83698	Cu	4.15	63.6	49.4	18.2	12.9	15.5		12.9	
			mean = 36.0(1,2)		25.2(1,3)		25.5(1,5)		20.5(1,6)	
			standard deviation = 1.3		2.3		2.3		1.6	
			Mean Base Strength Increment = 5.5		2.5		-0.2		0.4	

* Alloy base strength, see Tables 7 and 8 for definitions.

- NOTES: (1) Excludes precipitation and solid solution hardening alloying elements, Mg, Cu and Zn.
 (2) Unalloyed material room temperature mean base strength = 30.5 ksi.
 (3) Unalloyed material 450°F mean base strength = 22.7 ksi.
 (4) No influence of variations in dispersoid content on 550 or 650°F tensile properties has been observed.
 (5) Unalloyed material 550°F mean tensile strength = 25.7 ksi.
 (6) Unalloyed material 650°F mean tensile strength = 20.1 ksi.

Table 11. Contribution of Individual Alloying Elements
to R.T. Strength

Alloy Identification	Alloy Addition (Wt.%)	Alloy Addition (Vol.%)	Contribution to UTS (ksi)	Strength Change per Vol.% Added (ksi/Vol.%)
83074	1.79 Fe	0.62	4.6	7.4
83076	1.98 Co	0.61	4.2	6.9
83079	1.65 Ti	1.0	7.1	7.1
83081	1.09 Fe	0.38	6.1	16.1
83085	3.4 Mg	5.18	43.3	8.4
83086	1.92 Mn	0.71	6.7	9.4
83087	6.6 Zn	2.60	8.7	3.3
83696	1.60 Ni	0.49	3.9	8.0
83697	1.87 Cr	0.71	5.6	7.9
83698	3.9 Cu	1.21	18.9	15.6

Table 12. Tensile Properties - Ternary Alloys

Alloy Identification	Alloy Additions	v/o Dispersoid	R.T.				450°F				550°F				650°F			
			UTS (ksi)	YS (ksi)	El. (%)	RA (%)	UTS (ksi)	YS (ksi)	El. (%)	RA (%)	UTS (ksi)	YS (ksi)	El. (%)	RA (%)	UTS (ksi)	YS (ksi)	El. (%)	RA (%)
83700	1.75Fe-1.9Ti	4.2	54.0	46.4	7.0	22.0	32.4	26.9	4.0	4-9.5	27.6	24.0	2.5	4.5	21.6	19.0	3.0	6.0
83702	1.65Fe-1.68Cr	4.9	55.2	46.6	11.0	25.0	34.3	28.8	3.5	8.5	30.3	23.9	4.5	9.5	25.6	23.4	2.5	4.5
83703	1.77Fe-2.35Cr	4.4	54.8	47.8	10.0	28.0	33.6	28.6	2.0	6.0	29.2	24.7	4.0	5.5	23.8	21.4	1.5	1.8
83074	1.39Ti-1.82Cr	4.7	53.7	46.8	8.0	19.0	36.1	30.5	4.5	6-15	28.7	23.0	22.0	4.5	22.4	19.4	2.0	2.0
83089	4.0Ti	5.4	55.6	47.2	10.5	29.5	36.5	29.2	3.0	2-10	30.4	26.4	5.5	11.5	27.0	23.0	1-3	6-12

Table 13. Base Tensile Strength of Ternary Alloys at Various Temperatures

Alloy Identification	Addition	v/o Dispersoid	R.T.		450°F		550°F		650°F	
			UTS (ksi)	σ_o^* (ksi)	UTS (ksi)	σ_o^* (ksi)	UTS (ksi)	σ_o^* (ksi)	UTS (ksi)	σ_o^* (ksi)
83700	Fe-Ti	4.2	54.0	39.7	32.4	27.1	27.6	21.6	21.6	
83702	Fe-Cr	4.9	55.2	38.5	34.3	28.1	30.3	25.6	25.6	
83703	Fe-Cr	4.4	54.8	39.2	33.6	28.0	29.2	23.8	23.8	
83704	Ti-Cr	4.7	53.7	37.7	36.1	30.1	28.7	22.4	22.4	
83089	Ti	5.4	55.6	37.2	36.5	29.6	30.4	27.0	27.0	
			mean = 38.5		28.6		29.2		24.1	
			standard deviation = 1.0		1.2		1.2		2.2	
			Mean Base Strength Increment = 8.0		5.9		3.5		4.0	

* Alloy base strength, see Tables 7 and 8 for definitions.

Table 14. Effect of High Temperature Exposure on R.T. Tensile Properties

Alloy Identification	Alloying Element	None						Exposure					
		450°F-100 hr						650°F-100 hr					
		UTS (ksi)	YS (ksi)	El. (%)	RA (%)	UTS (ksi)	YS (ksi)	El. (%)	RA (%)	UTS (ksi)	YS (ksi)	El. (%)	RA (%)
83060	-	51.8	46.3	6.0	60.0	52.9	48.1	15.0	53.5	52.8	48.0	14.5	54.0
83062	-	55.5	50.7	5.5	17.5	55.2	50.9	6.5	16.8	54.3	49.9	5.5	19.0
83071	-	47.7	39.9	12.0	44.0	47.4	40.4	10.0	38.5	47.4	39.0	10.0	35.5
83072	-	60.6	55.5	8.0	32.8	59.4	54.7	7.0	32.5	60.8	54.7	6.3	34.5
83073	-	56.5	50.5	5.5	17.5	57.3	52.0	5.5	17.5	56.4	50.2	6.5	19.0
83088	-	59.5	53.4	9.0	36.0	59.7	54.9	5.5	36.0	62.3	55.6	7.5	36.5
83074	Fe	50.0	41.5	11.0	30.5	48.9	42.9	5.5	30.5	49.0	41.7	6.0	26.5
83076	Co	49.4	42.4	17.5	57.5	48.5	42.3	16.0	54.0	47.6	42.4	16.0	57.0
83079	Ti	52.4	45.8	11.5	48.0	52.3	45.0	13.0	42.0	51.5	44.8	11.5	41.0
83081	Fe	55.6	48.2	9.5	30.5	54.4	48.2	9.5	28.0	54.0	48.4	9.5	26.5
83085	Mg	89.0	78.5	6.0	30.0	87.9	80.5	5.5	19.5	88.4	80.5	5.5	19.0
83086	Mn	52.8	44.7	10.5	28.5	50.7	45.7	10.0	26.5	50.4	44.0	9.5	28.0
83087	Zn	56.5	49.6	9.0	27.5	54.8	47.9	9.0	26.0	54.1	45.8	9.5	24.0
83696	Ni	49.0	41.2	15.0	47.0	48.6	41.5	16.5	46.0	49.9	42.0	15.5	44.0
83697	Cr	48.4	42.6	9.5	31.0	48.4	43.6	13.0	37.0	48.8	42.5	11.5	33.5
83698	Cu	63.6	55.3	8.5	17.0	62.5	55.9	8.0	20.5	63.8	56.6	9.5	20.5
83700	Fe+Ti	54.0	46.4	7.0	22.0	52.1	47.3	6.5	19.0	51.5	45.4	8.5	20.0
83702	Fe+Cr	55.2	46.6	11.0	25.0	53.2	43.4	10.0	31.0	52.4	46.4	11.0	24.5
83703	Fe+Cr	54.8	47.8	10.0	28.0	54.5	49.7	8.5	27.5	54.3	48.3	8.0	23.0
83704	Cr+Ti	53.7	46.8	8.0	19.0	51.6	46.6	6.0	17.0	49.0	41.8	6.5	15.5
83089	Ti	55.6	47.2	10.5	29.5	54.9	48.3	9.5	27.0	54.1	46.4	11.0	27.5

Table 15. Stress-Rupture Data - Unalloyed Materials.

Alloy Identification	v/o Dispersoid	(Carbide/Oxide) by Volume	Test Temp. (°F)	Stress (ksi)	Life (hr)	El. (%)	RA (%)
83060	6.95	1.99	450	18	8.9	0	0
			450	18	5.2	0	0
			650	17	2.3	1	3.2
			650	16	.5	0	0
83062	8.10	.98	450	20	2.4	0	0*
			650	17	1.4	0	0
83071	4.96	.66	450	22	20.6	3	2
			450	22	28.1	1.3	1.2
			650	17	.8	1	0
			650	16	1.7	1	0
83072	8.80	3.00	450	20	6.5	0	0*
			650	12	.3	0	0
83073	8.47	.90	450	22	4.4	0	0*
			450	22	10.0	0	0*
			650	17	0.6	0	0*
			650	16	2656.0	Nil	Nil**
83088	7.33	2.37	450	18	.3	0	0*
			650	18	1.9	2	6.3
			650	17	.1	1	1.2

* Broke through threads.

** Unbroken, test terminated.

Table 16. Stress-Rupture Data - Binary Alloys.

Alloy Identification	Alloy Addition	v/o Dispersoid	Test Temp. (°F)	Stress (ksi)	Life (hr)	El. (%)	RA (%)
83074-7	1.79 Fe	4.23	450	24	1.3	2	3.8
-9	1.79 Fe	4.23	450	22	25.0	1	1.4
-8	1.79 Fe	4.23	650	15	14.1	3	2.8
-10	1.79 Fe	4.23	650	15	.6	1	1
83076-7	1.98 Co	4.30	450	22	4.2	2	10.4
-9	1.98 Co	4.30	450	22	2.9	13	9.7
-8	1.98 Co	4.30	650	16	1.4	5	12.8
-10	1.98 Co	4.30	650	15	227.8	1	18
83079-7	1.65 Ti	4.34	450	28	4	3	6.5
-9	1.65 Ti	4.34	450	26	20.5	4	11.5
-8	1.65 Ti	4.34	650	17	30.7	4	10
-10	1.65 Ti	4.34	650	17	150.1	2	6.6
83081-7	1.09 Fe	5.56	450	18	9.2	Nil	Nil*
-9	1.09 Fe	5.56	450	18	25.9	Nil	Nil*
-8	1.09 Fe	5.56	650	19	7.1	3	9.4
-10	1.09 Fe	5.56	650	19	.7	3	4.0
83085-7	3.4 Mg	4.46	450	18	.3	29	78.2
-9	3.4 Mg	4.46	450	16	1.2	23	79.1
-8	3.4 Mg	4.46	650	10	12.2	8	30.2
-10	3.4 Mg	4.46	650	10	12.3	8	37
83086-7	1.92 Mn	4.58	450	20	7.9	Nil	Nil*
-9	1.92 Mn	4.58	450	20	14.2	Nil	Nil
-8	1.92 Mn	4.58	650	15	4.9	Nil	Nil
83087-7	6.6 Zn	5.07	450	18	6.1	Nil	Nil*
-9	6.6 Zn	5.07	450	18	13.0	2	5.2
-8	6.6 Zn	5.07	650	14	.9	0	0*
-10	6.6 Zn	5.07	650	9	2200	Nil	Nil**
83696-7	1.6 Ni	4.29	450	24	1.0	3	12
-9	1.6 Ni	4.29	450	22	34.2	3	10.1
-8	1.6 Ni	4.29	650	18	21.3	7	22
-10	1.6 Ni	4.29	650	18	2.7	6	16.2
83697-7	1.87 Cr	3.60	450	24	3.6	0	0*
-9	1.87 Cr	3.60	450	22	43.4	0	0*
-8	1.87 Cr	3.60	650	15	26.3	3	9.9
-10	1.87 Cr	3.60	650	16	2.6	4	14.8
83698-7	3.6 Cu	4.15	450	18	26.3	4	14.7
-9	3.6 Cu	4.15	450	18	32.4	4	17.7
-8	3.6 Cu	4.15	650	13	11.1	4	4.4
-10	3.6 Cu	4.15	650	13	1.4	9	24

* Broke through threads.

** Unbroken, test terminated.

Table 17. Stress-Rupture Data - Ternary Alloys.

Alloy Identification	Alloy Addition	V/O Dispersoid	Test Temp. (°F)	Stress (ksi)	Life (hr)	El. (%)	RA (%)	Comments
83700	1.75Fe-1.9Ti	4.17	450	28	5.4	2.0	Nil	
			450	28	5.2	1.0	1.2	
			450	25	173.8	2.0	Nil	
			650	13.5/14	358.5/1.8	Nil	Nil	
			650	15	15	2.0	"	
83702	1.65Fe-1.68Cr	4.91	650	15	15	1.0	4.0	
			450	26	15.1	Nil	Nil	Failed in Head Twice
			450	29	3.7	"	"	Head Failure
			450	26	29.4	"	"	"
			650	19	8.7	1.0	Nil	
83703	1.77Fe-2.35Cr	4.45	650	19.5	11.2	2.0	Nil*	
			650	18	1.8	Nil	Nil	
			450	24	1.6	Nil	Nil	Failed in Head Twice
			450	22	526.4	"	"	Unbroken, test terminated
			450	24	599.8	"	"	Unbroken, test terminated
83704	1.82Cr-1.39Ti	4.70	650	18	14.1	1.0	Nil	
			650	16.5	2.1	Nil	"	
			650	15	98.1	1.0	Nil*	Head Failure
			450	28	5.7	2.0	2.5	
			450	27	11.6	1.0	1.4	
83089	4Ti	5.35	450	25	289.3	Nil	Nil	
			650	16	5.2	1.0	Nil	
			650	16	11.3	1.0	"	
			650	13.5	376.0	1.0	"	
			450	28	23.4	2.0	2.0	
83089	4Ti	5.35	450	28	6.0	2.0	5.5	
			450	24	37.9	1.0	Nil	
			450	30	10.6	2.0	2.5*	
			650	19	22.8	1.0	Nil	
			650	17.5	166.0	1.0	"	

* Highest applied stress, step loaded for creep test.

Table 18. Values of ϵ_I and $\dot{\epsilon}_S$ Obtained from 450°F Creep Tests.

Alloy Identification	Alloy Addition	Stress (ksi)	Primary Creep Strain (ϵ_I)	Steady-State Creep Rate ($\dot{\epsilon}_S$)
83700	1.75Fe-1.9Ti	23	0.0010	8.75×10^{-6}
		25	-	1.74×10^{-5}
83702	1.65Fe-1.68Cr	24	0.0014	1.82×10^{-6}
		25	-	2.00×10^{-6}
		26	-	6.00×10^{-6}
		27	-	1.5×10^{-6}
83704	1.82Cr-1.39Ti	25	0.0028	1.04×10^{-5}
83089	4Ti	24	0.0008	$1.76-2.29 \times 10^{-5}$
		22	0.0014	2.26×10^{-6}
		24	-	1.2×10^{-5}
		26	-	1.6×10^{-5}
		28	-	4.26×10^{-5}

Table 19. Values of ϵ_I and $\dot{\epsilon}_S$ Obtained from 650°F Creep Tests.

Alloy Identification	Alloy Addition	Stress (ksi)	Primary Creep Strain (ϵ_I)	Steady-State Creep Rate (hr ⁻¹) ($\dot{\epsilon}_S$)
83700	1.75Fe-1.9Ti	13.5	0.0029	2.5×10^{-6}
83702	1.65Fe-1.68Cr	13.5	0.0016	5.5×10^{-6}
		15	-	1.9×10^{-6}
		16.5	-	3×10^{-6}
		18	-	1.2×10^{-6}
83703	1.77Fe-2.35Cr	13.5	0.0	9×10^{-6}
		14.5		3.6×10^{-6}
		17		1.6×10^{-5}
83704	1.82Cr-1.39Ti	13.5	0.0005	5.3×10^{-6}
		15	-	9×10^{-6}
83089	4Ti	11	0.0004	3.5×10^{-5}
		12	-	5.2×10^{-6}
		17.5	0.0020	1.8×10^{-5}

Thermomechanical

Alloy Identification	Processing Variations	Test Temperature															
		70°F				450°F				550°F				650°F			
		UTS (ksi)	YS (ksi)	El. (%)	RA (%)	UTS (ksi)	YS (ksi)	El. (%)	RA (%)	UTS (ksi)	YS (ksi)	El. (%)	RA (%)	UTS (ksi)	YS (ksi)	El. (%)	RA (%)
83060(2)	None	51.8	46.3	6	60	31.6	27.6	4.5	16	26.4	23.7	2	3	19.9	-	1	0
	750	49.9	42.9	14.5	52												
	750	48.6	37.9	12	41.5	29.4	25.8	9	36	24.4	21.0	9	38	20.0	19.3	6.5	27.5
	950	48.8	40.9	15.5	57												
	950	48.0	38.5	14.5	45	29.1	25.6	9	34.5	23.6	21.0	8	34.5	19.7	18.6	5.5	28

NOTES: (1) Hot roll from 5/8 inch round bar to 5/16 inch in 14 passes.
(2) 6.95 vol.% dispersed.

Table 21. Effect of Modified Thermomechanical Processing on Stress-Rupture Properties of Unalloyed Al.

Processing	Stress Rupture Properties							
	450°F				650°F			
	Stress (ksi)	Life (hrs)	El. (%)	RA (%)	Stress (ksi)	Life (hrs)	El. (%)	RA (%)
Standard	18	5.2	Head Failure		17	2.3	1	3.2
	18	8.9	Head Failure		16	0.5	0	0
Modified TMP	20	118.2	1.3	0	14	21.1	2.5	3.3
	21	30.0	1.3	3.4	15	21.3	5.0	14.0
	22	17.1	2.5	2.7	16	3.3	2.5	7.2
	22	12.6	3.8	2.7	16	12.8	3.8	8.0

Table 22. Effect of Thermomechanical Processing Variations on the Properties of MA Al-4Ti.

Extrusion Parameters		Tensile Properties											
		Room Temp.						450°F					
Temp. (°F)	Strain Rate (sec-1)	UTS (ksi)	YS (ksi)	El. (%)	RA (%)	UTS (ksi)	YS (ksi)	El. (%)	RA (%)	UTS (ksi)	YS (ksi)	El. (%)	RA (%)
800	10	55.6	47.2	10.5	29.5	36.5	29.2	3.0	2-10	27.0	23.0	1-3	6-12
1050	2	37.7	35.4	12.0	22.0	30.4	26.4	7.0	19.5	23.5	21.0	1.0*	5.0*

* Possible defect.

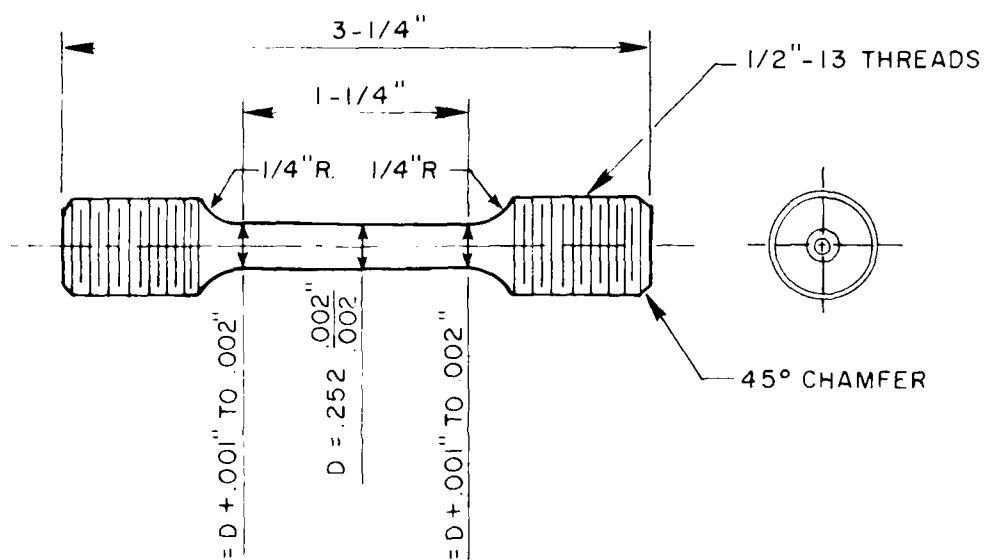


FIGURE 1-ROOM AND ELEVATED TEMPERATURE TEST SPECIMEN.

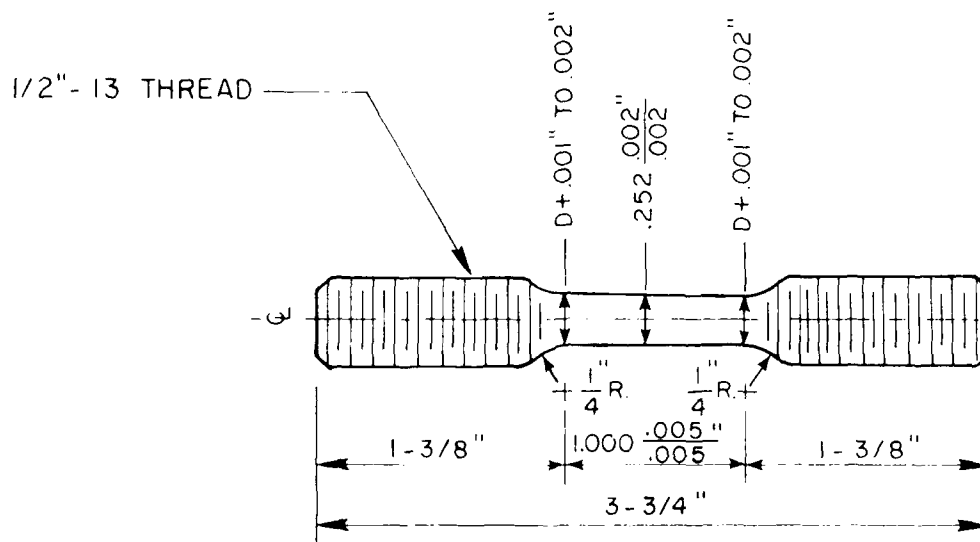


FIGURE 2 - STRESS-RUPTURE AND CREEP TEST SPECIMEN.

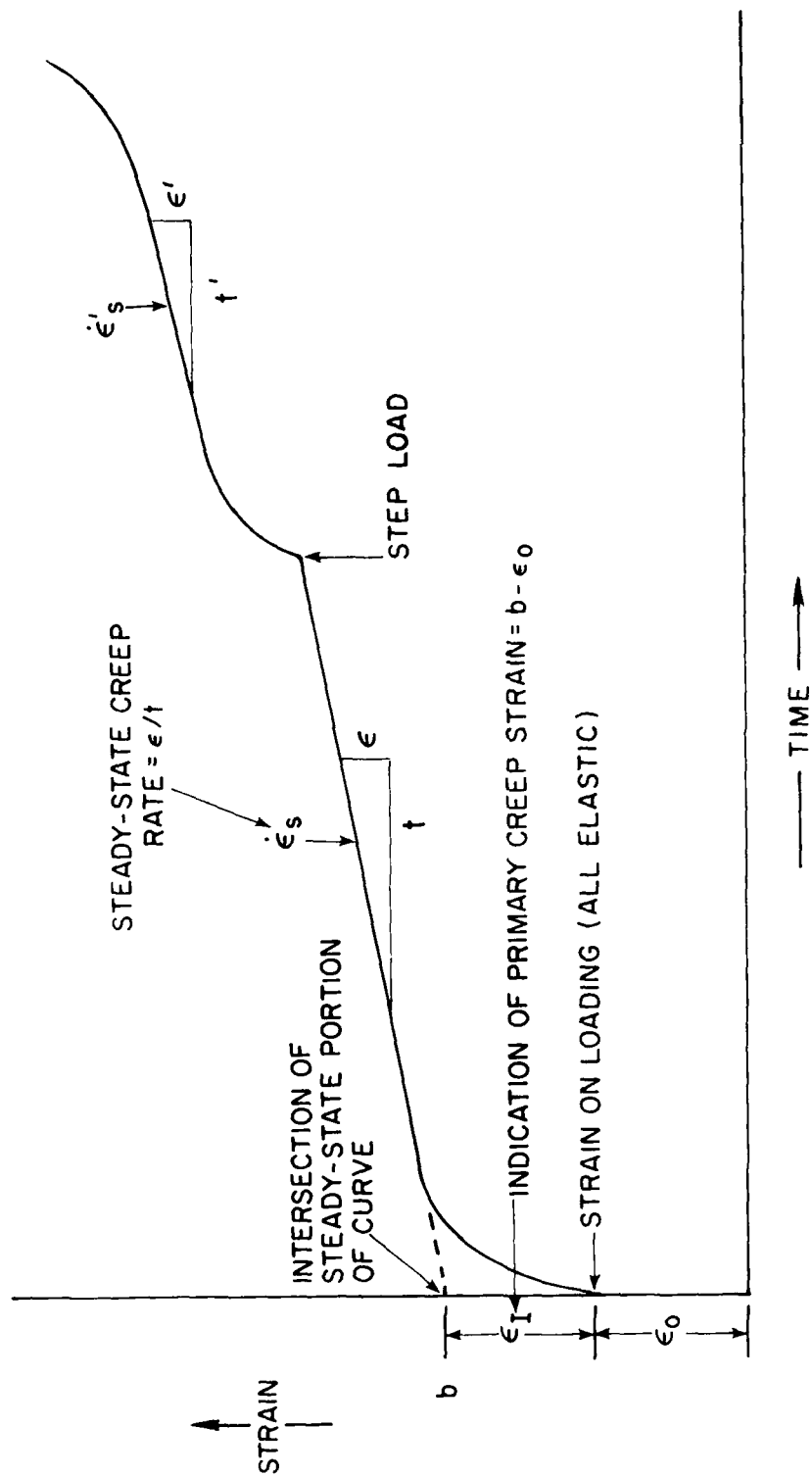


FIGURE 3 - SCHEMATIC REPRESENTATION OF TEST VALUES OBTAINED FROM A CREEP CURVE.

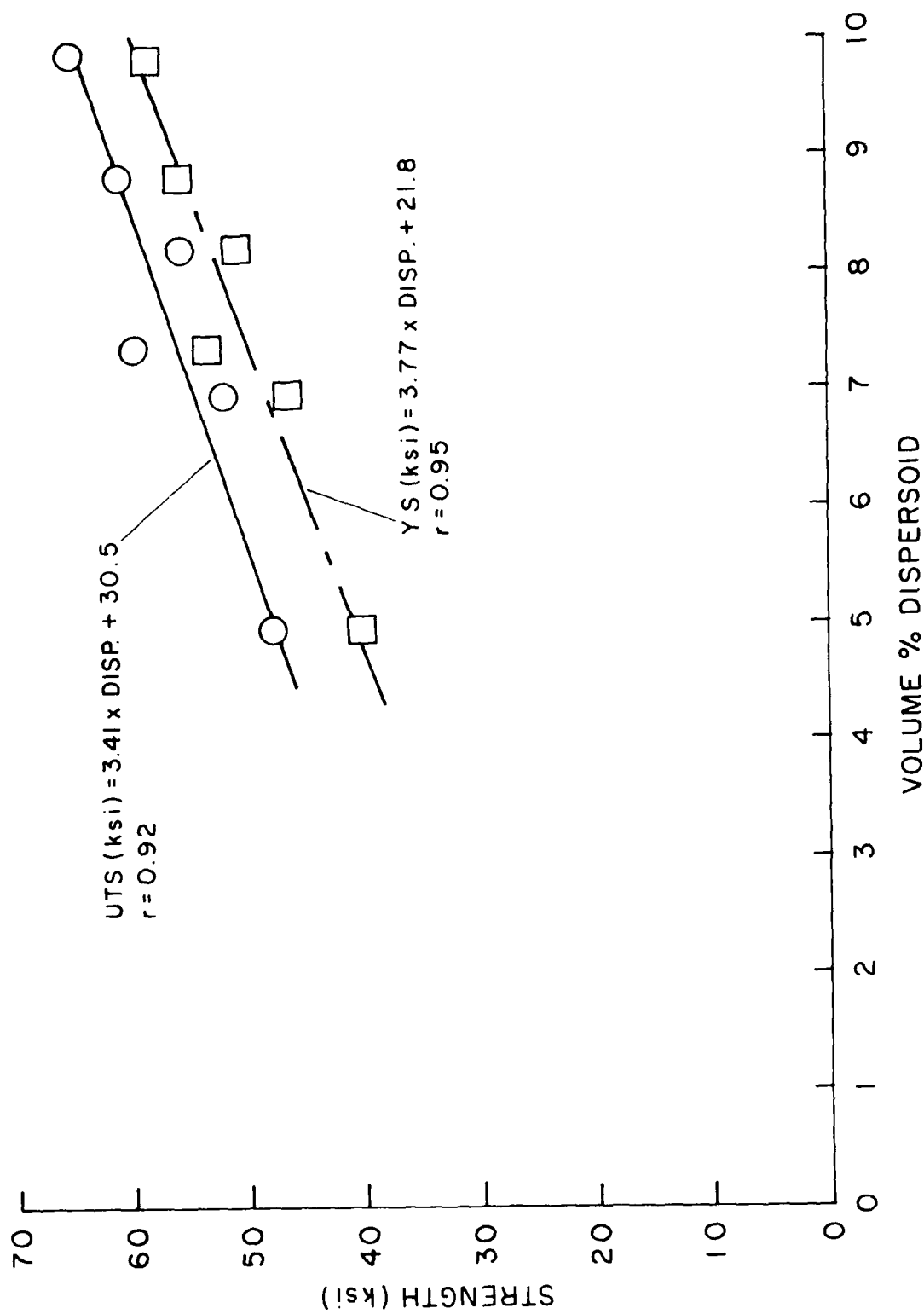


FIGURE 4 - STRENGTH AS A FUNCTION OF DISPERSOID CONTENT IN UNALLOYED MATERIAL.

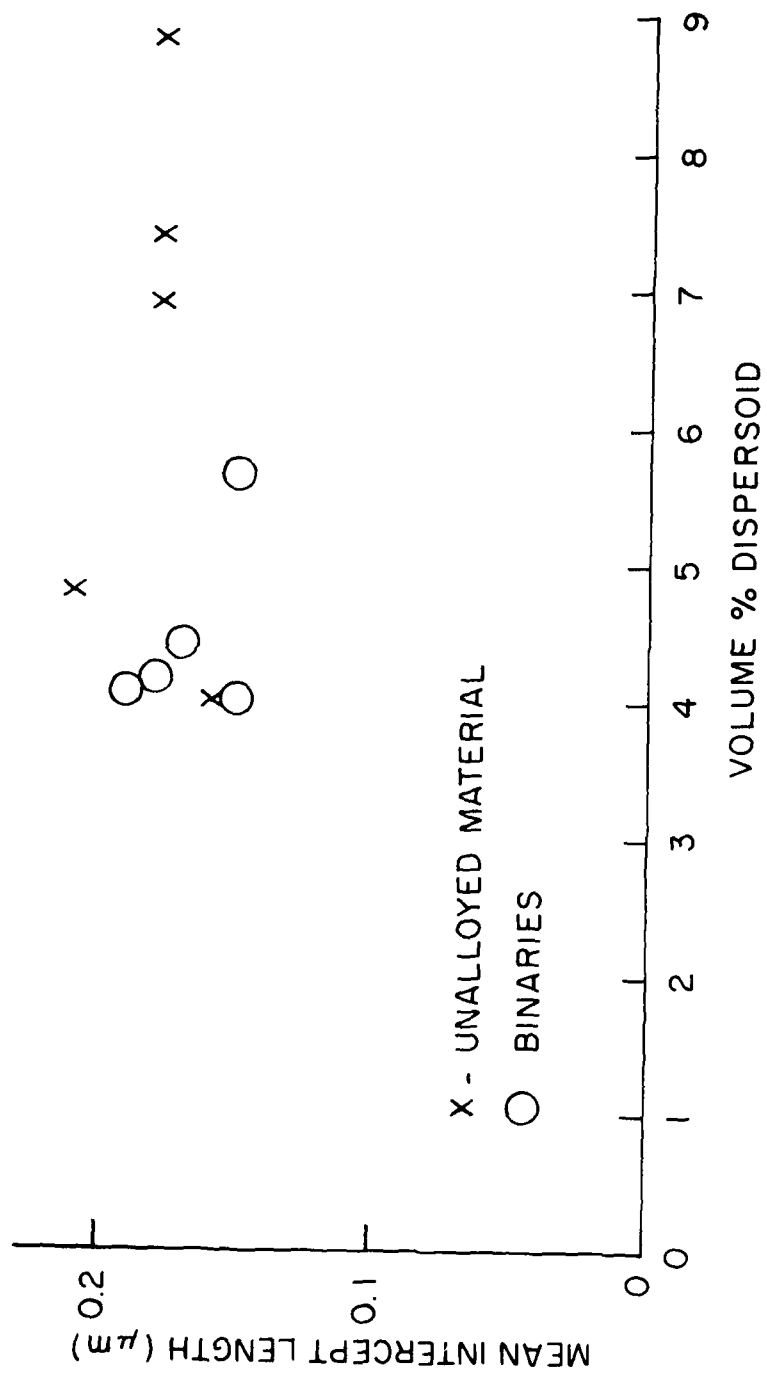


FIGURE - 5 GRAIN SIZE AS A FUNCTION OF VOLUME % DISPERSOID.

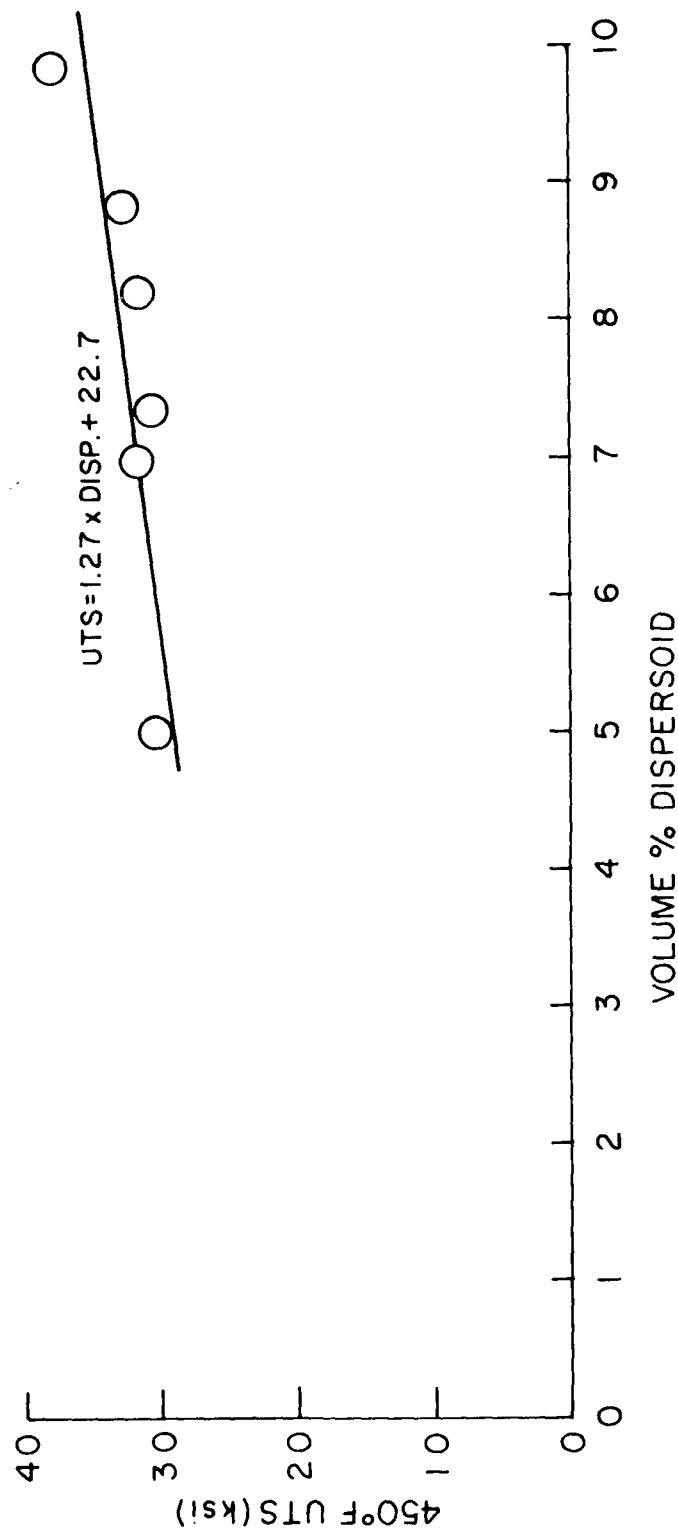


FIGURE 6 - EFFECT OF VOLUME % DISPERSOID ON 450°F ULTIMATE TENSILE STRENGTH - UNALLOYED MATERIAL.

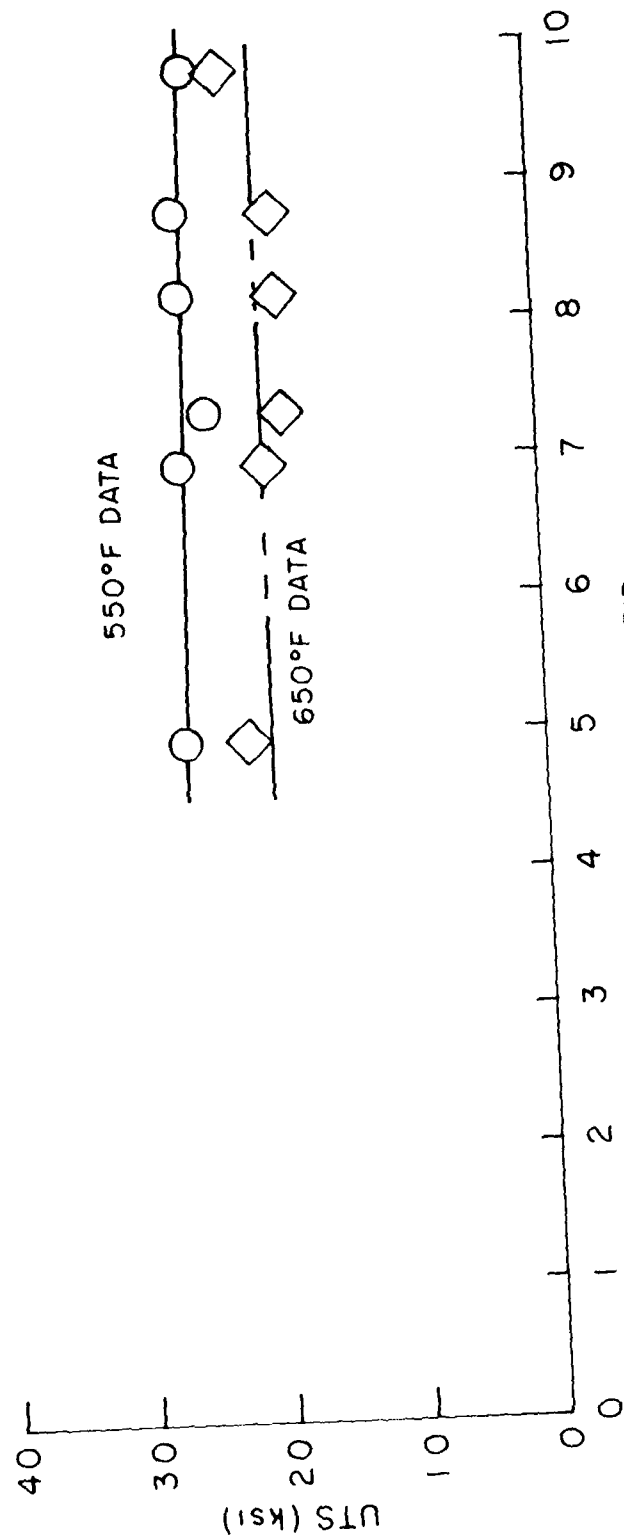


FIGURE 7 - EFFECT OF VOLUME % DISPERSOID ON 550°F AND 650°F ULTIMATE TENSILE STRENGTH - UNALLOYED MATERIAL.

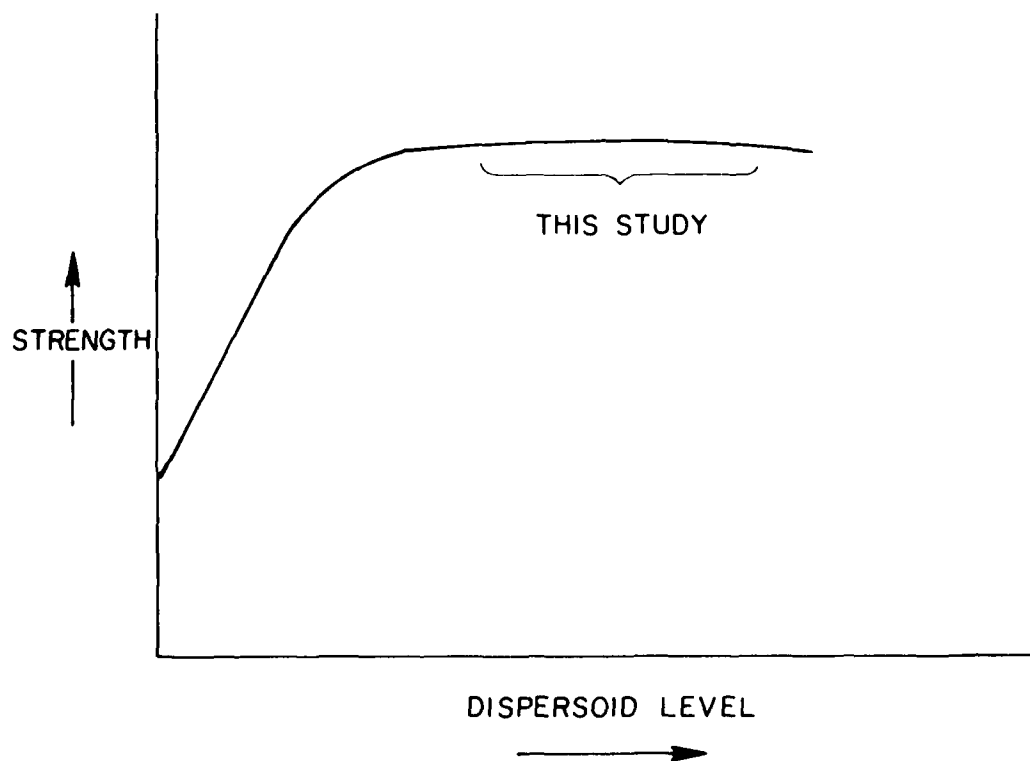


FIGURE 8 - EXPECTED HIGH TEMPERATURE ($\approx 550^{\circ}\text{F}$) STRENGTH
DEPENDENCE ON DISPERSOID CONTENT.

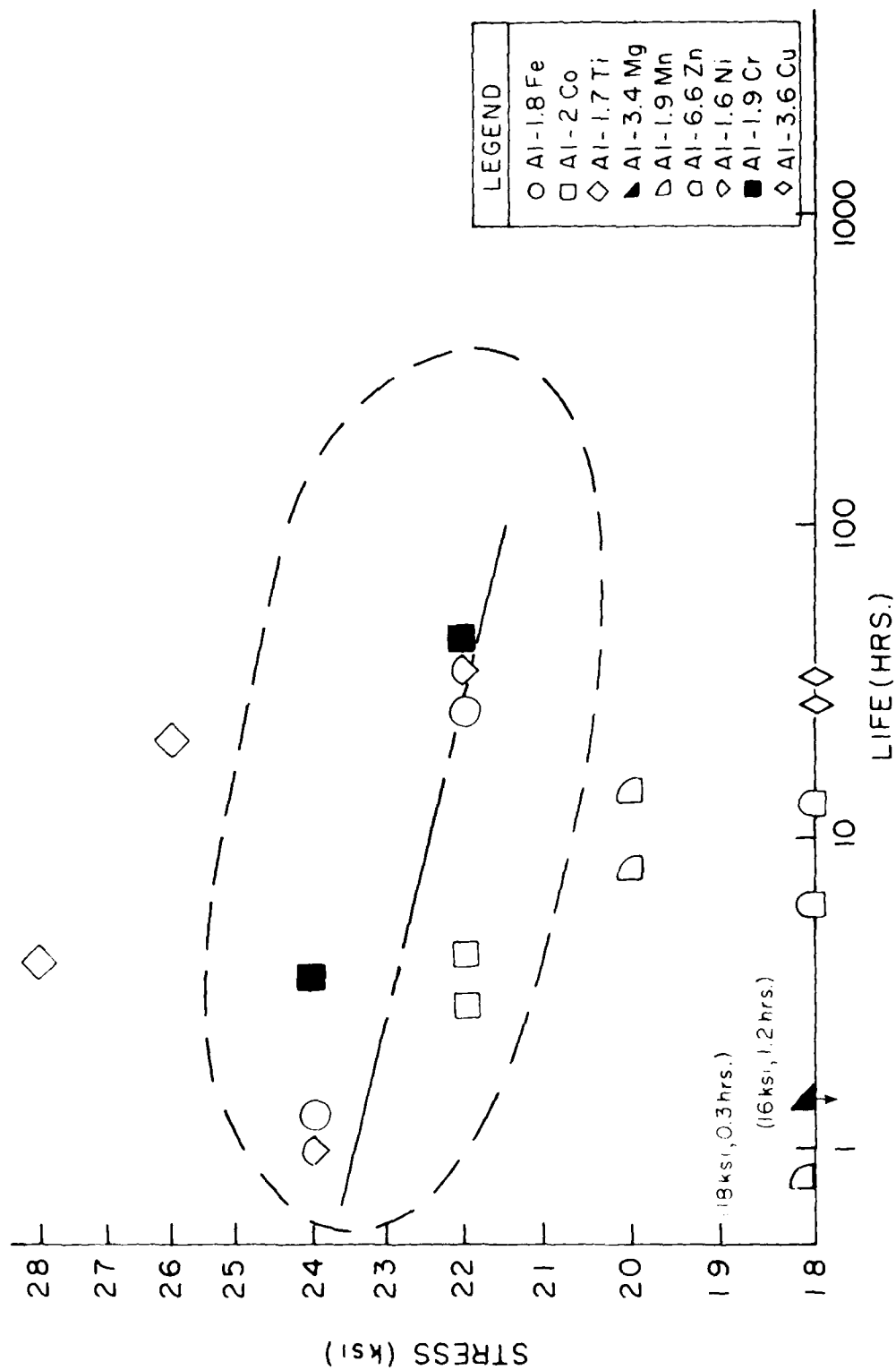


FIGURE 9 - BINARY ALLOYS - 450°F STRESS RUPTURE PROPERTIES.

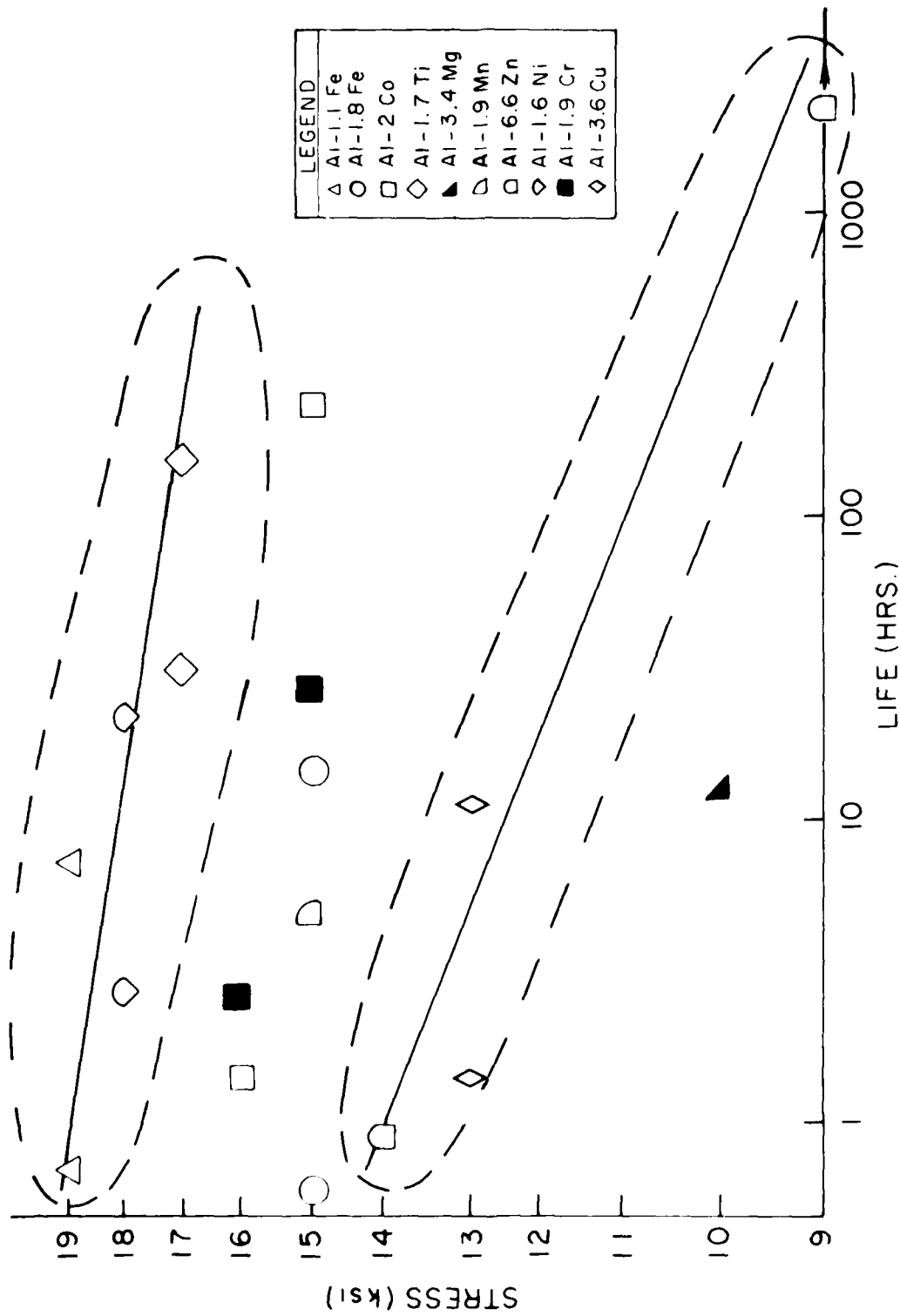


FIGURE 10 - BINARY ALLOYS - 650°F STRESS RUPTURE PROPERTIES.

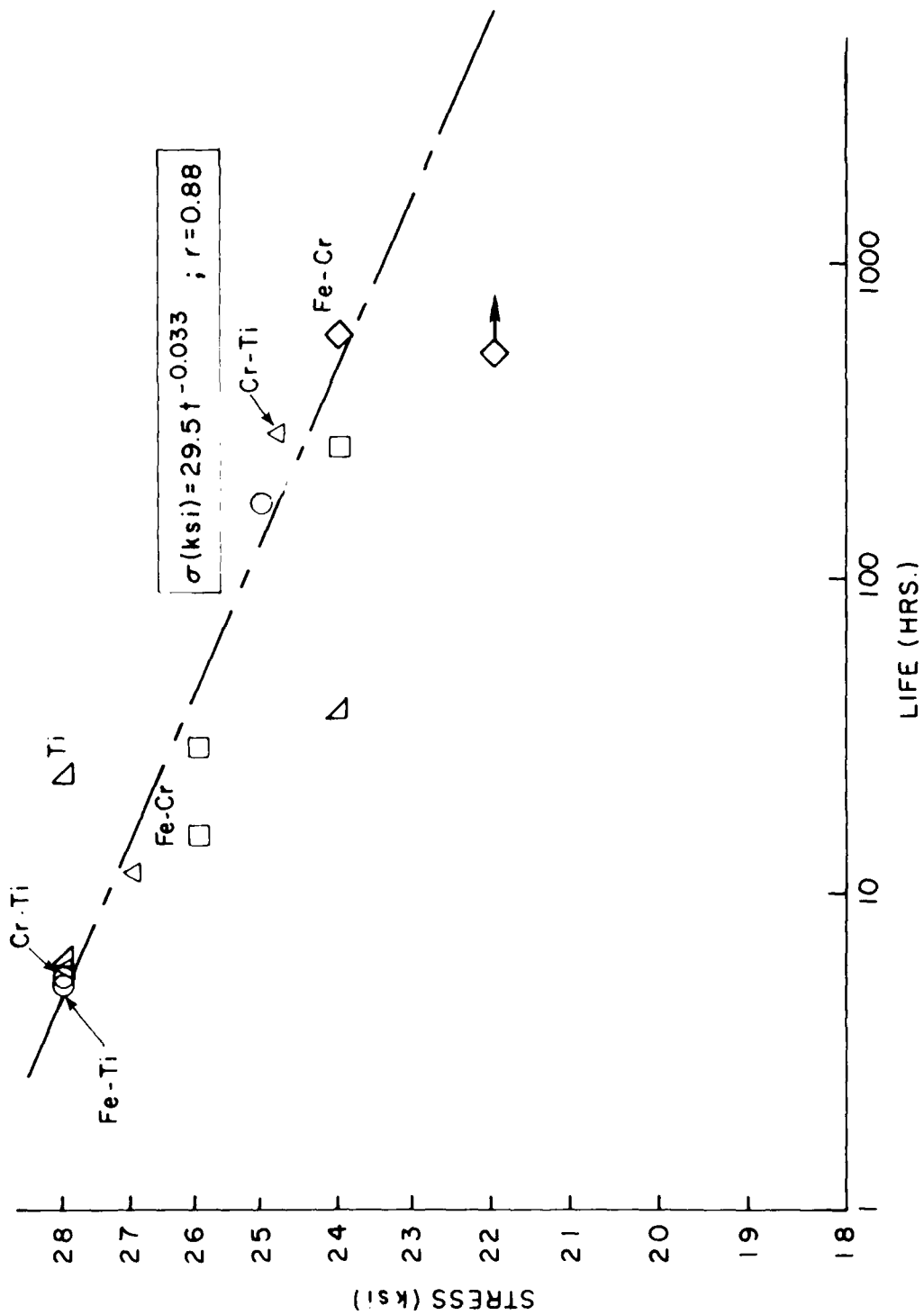


FIGURE II - TERNARY ALLOYS - 450°F STRESS RUPTURE PROPERTIES.

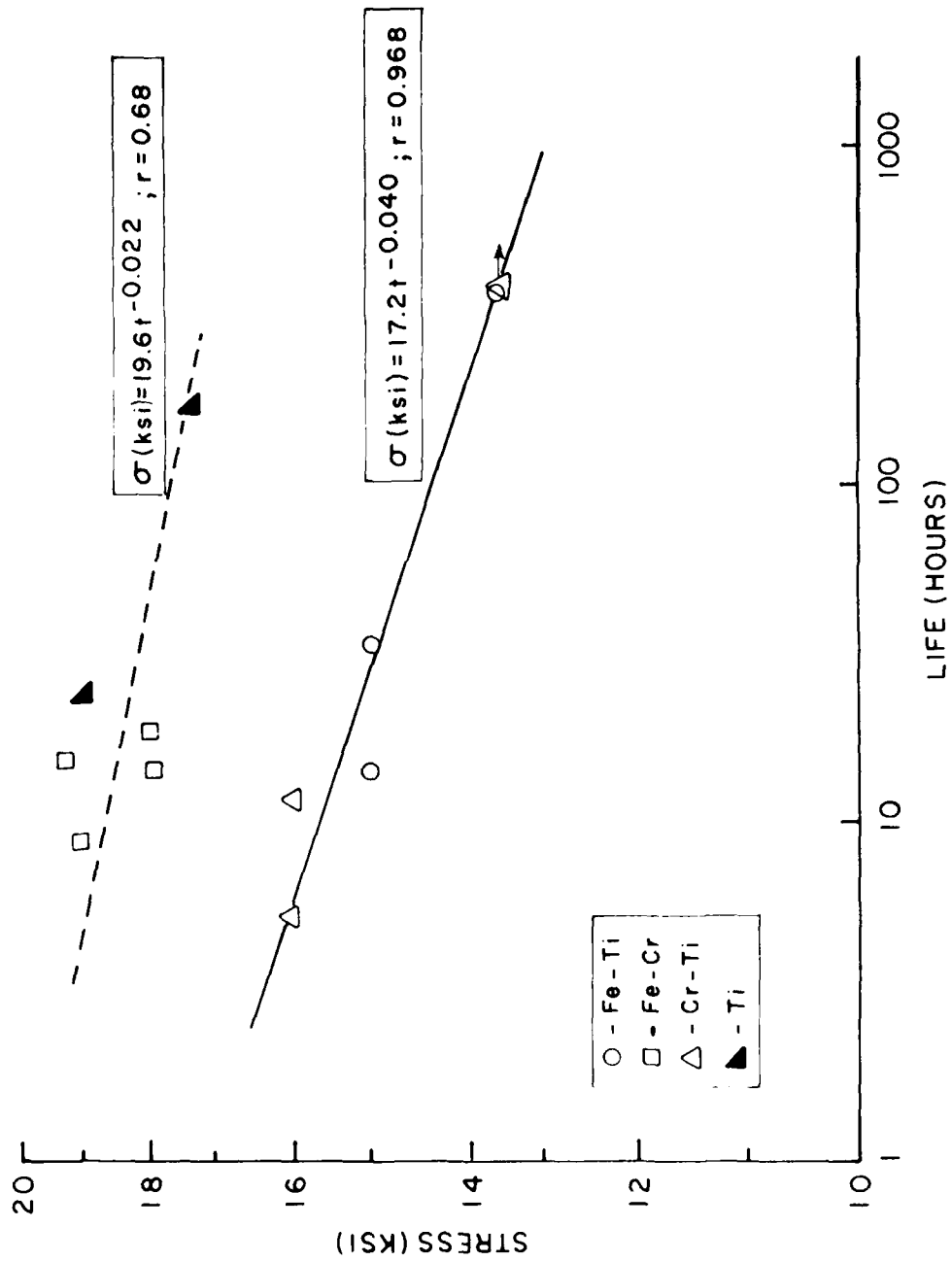


FIGURE 12- TERNARY ALLOYS - 650°F STRESS RUPTURE PROPERTIES.

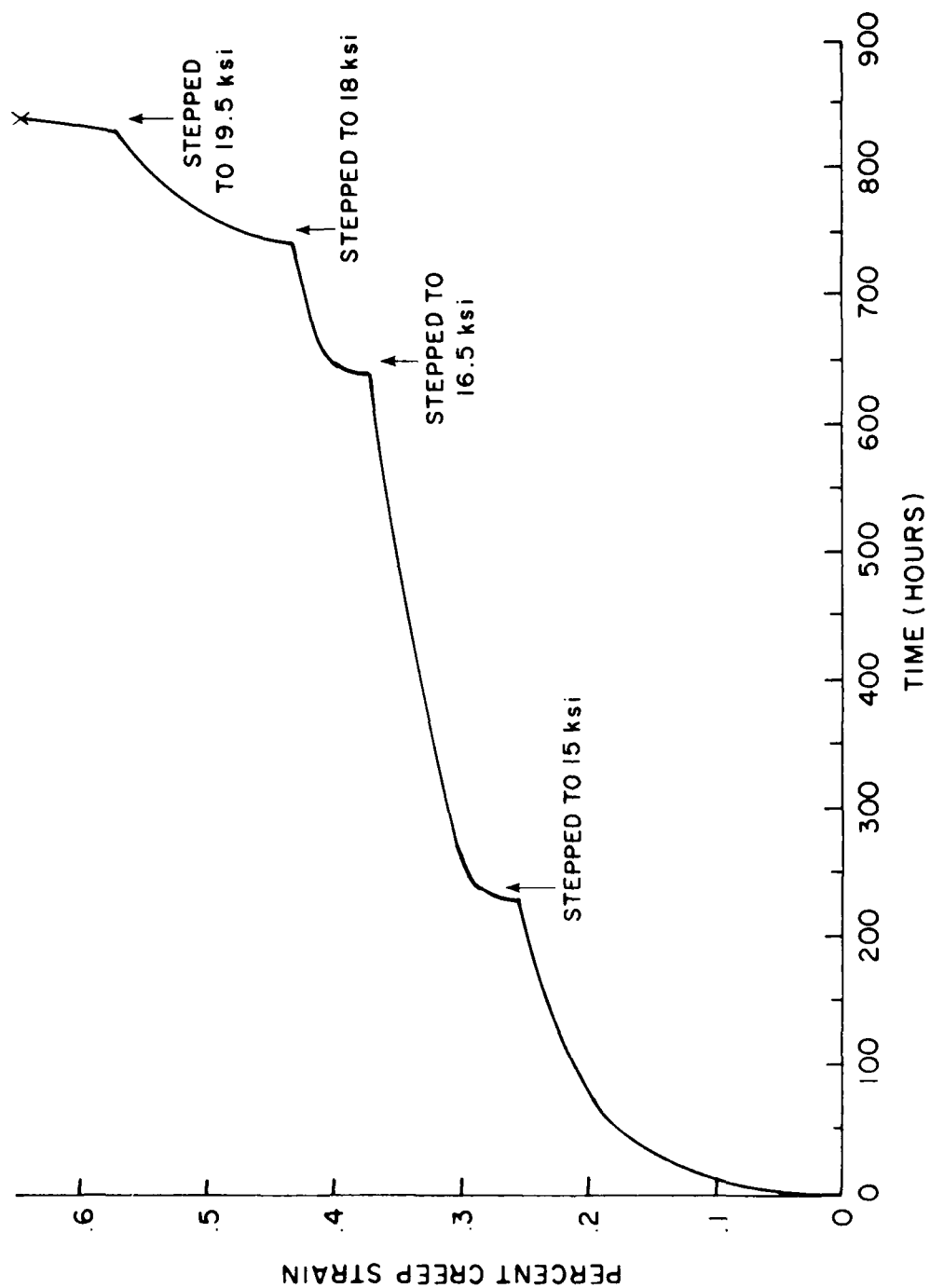


FIGURE 13 - TYPICAL CREEP RESPONSE FOR MA AL ALLOYS.

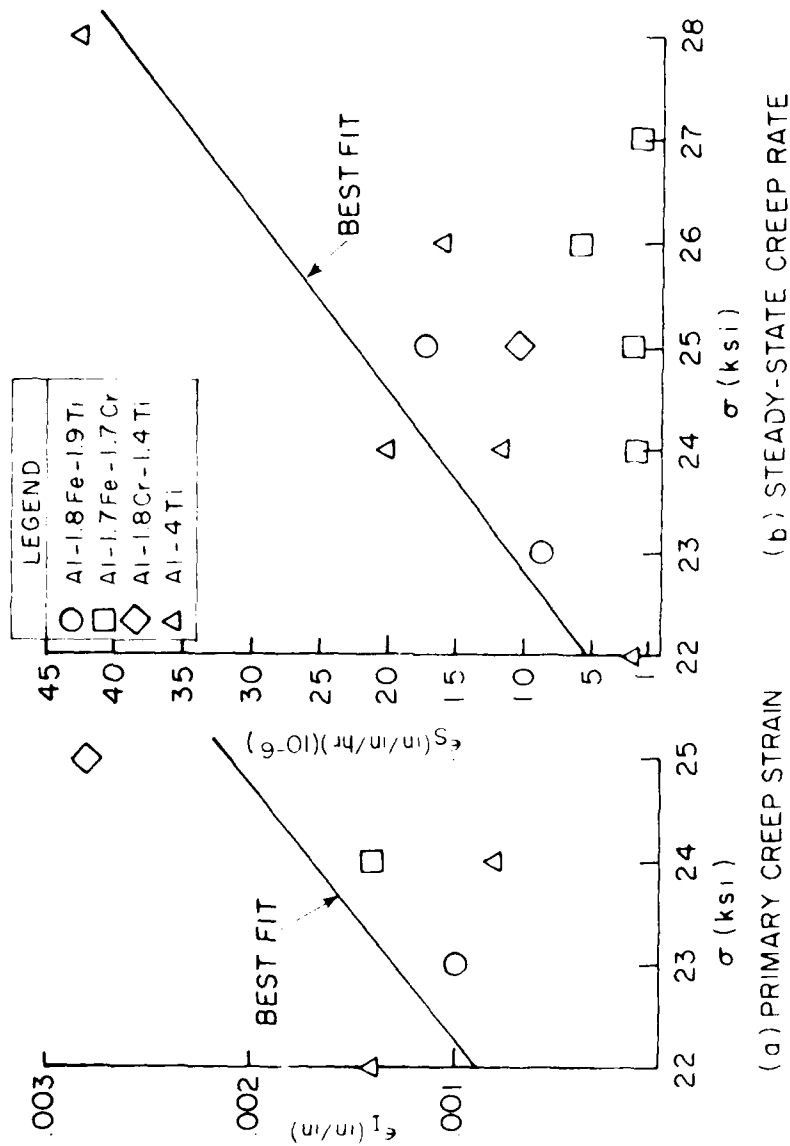


FIGURE 14 - VALUES OF ϵ_1 AND $\dot{\epsilon}_s$ AS A FUNCTION OF STRESS FOR 450°F CREEP TESTS.

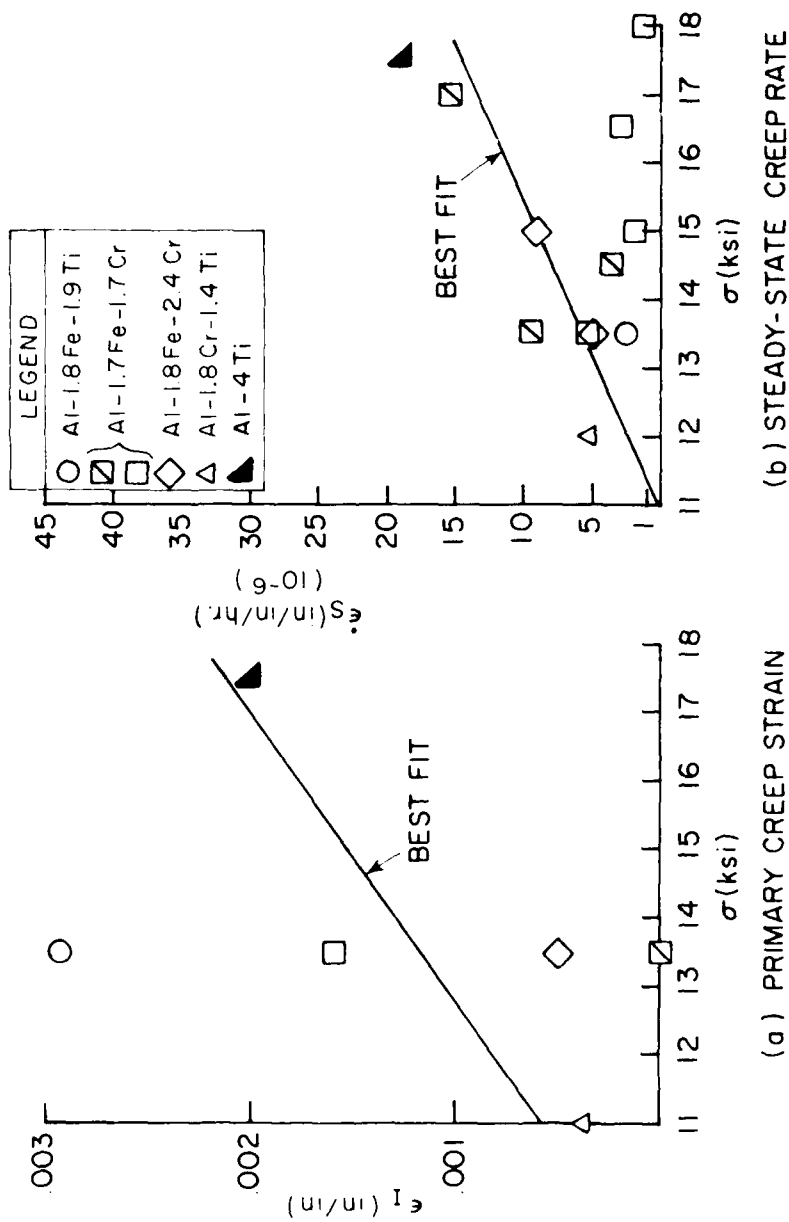


FIGURE 15 - VALUES OF ϵ_1 AND $\dot{\epsilon}_s$ AS A FUNCTION OF STRESS FOR 650°F CREEP TESTS.

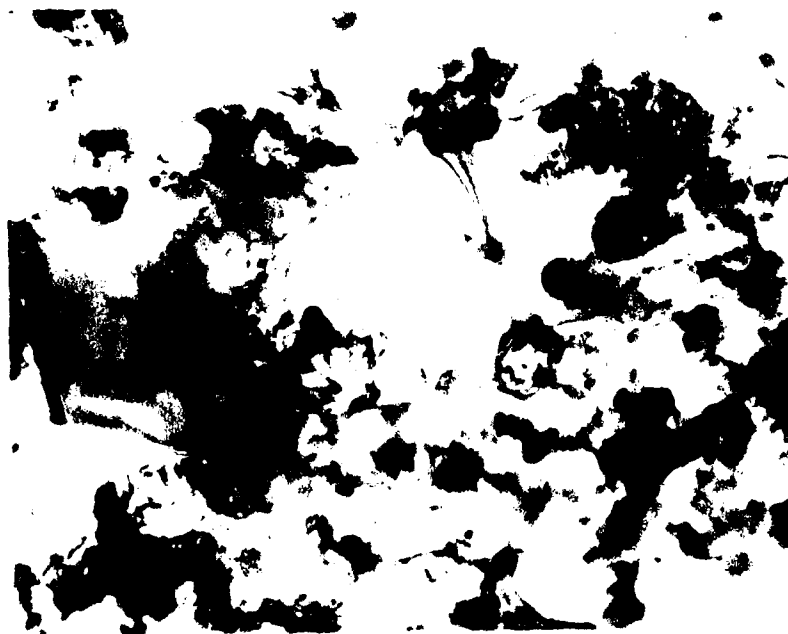
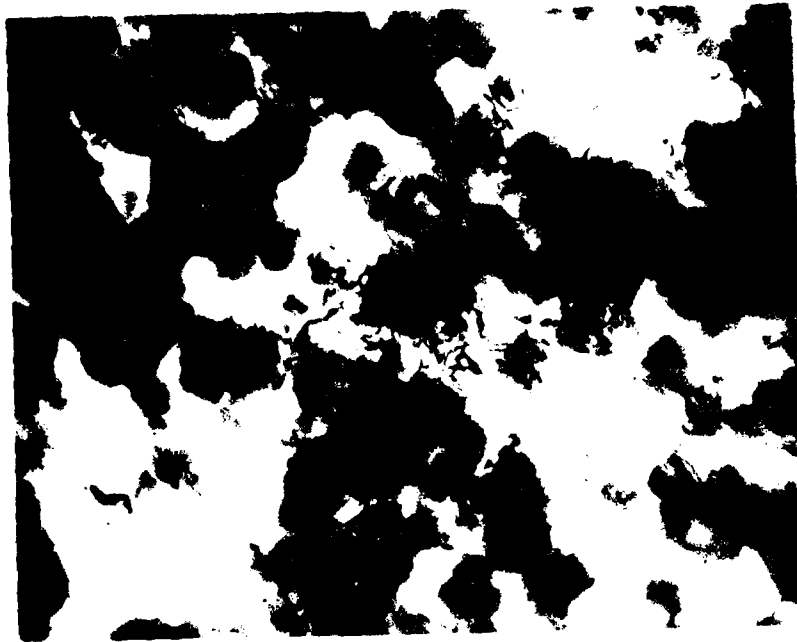


FIGURE 16: GRAIN AND CLUSTER OF POLLEN GRAINS, *POACEAE*,
LOW MAGNIFICATION, EXTENDED.

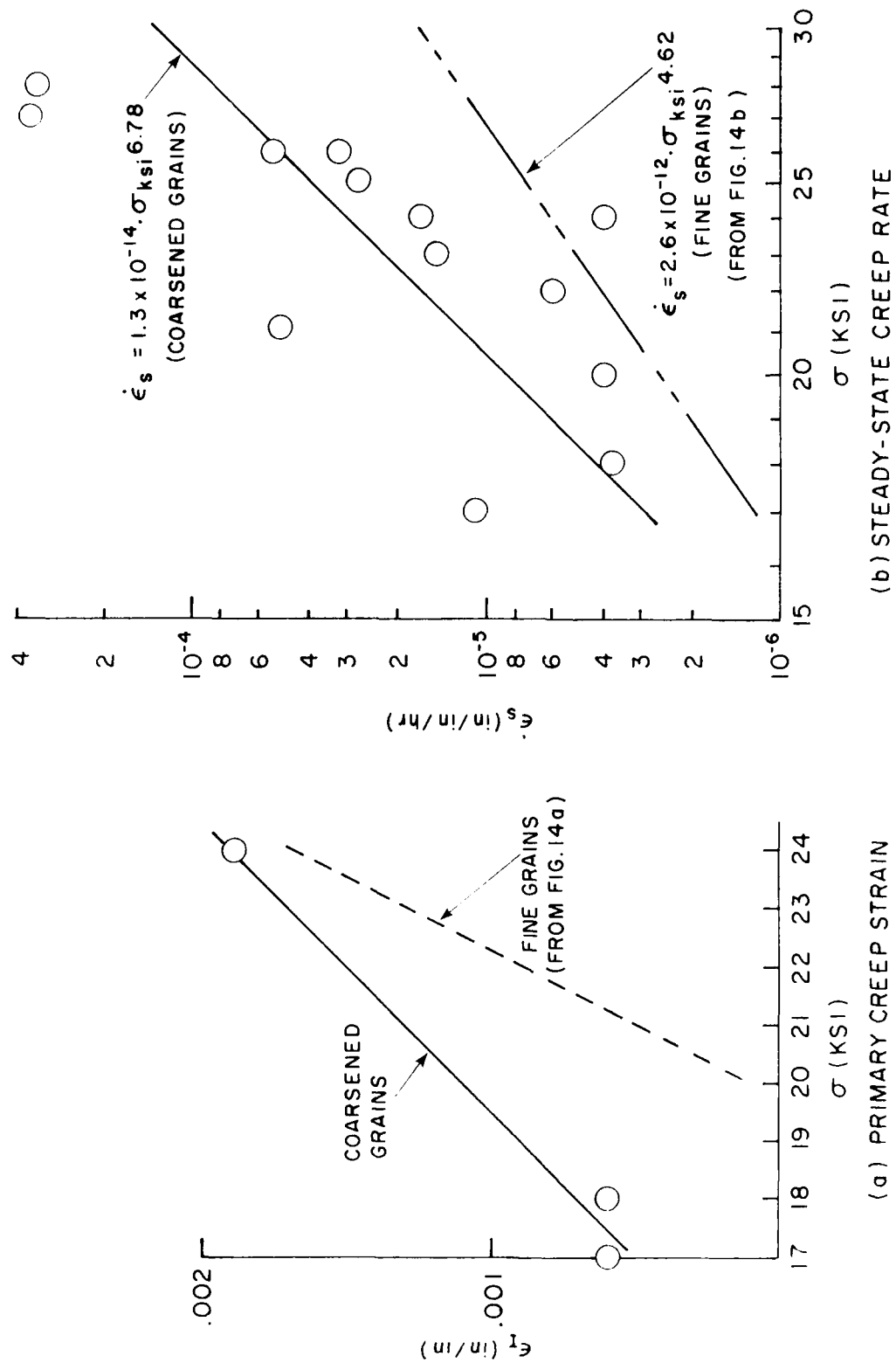
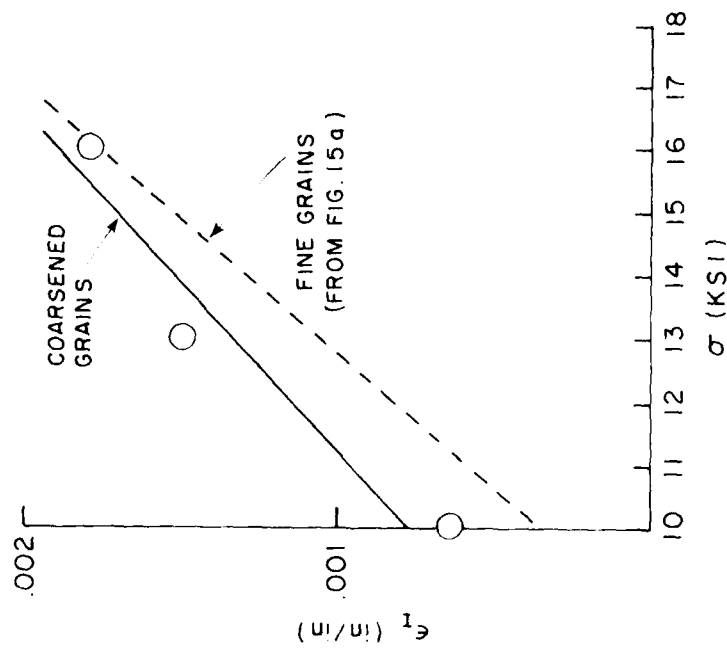
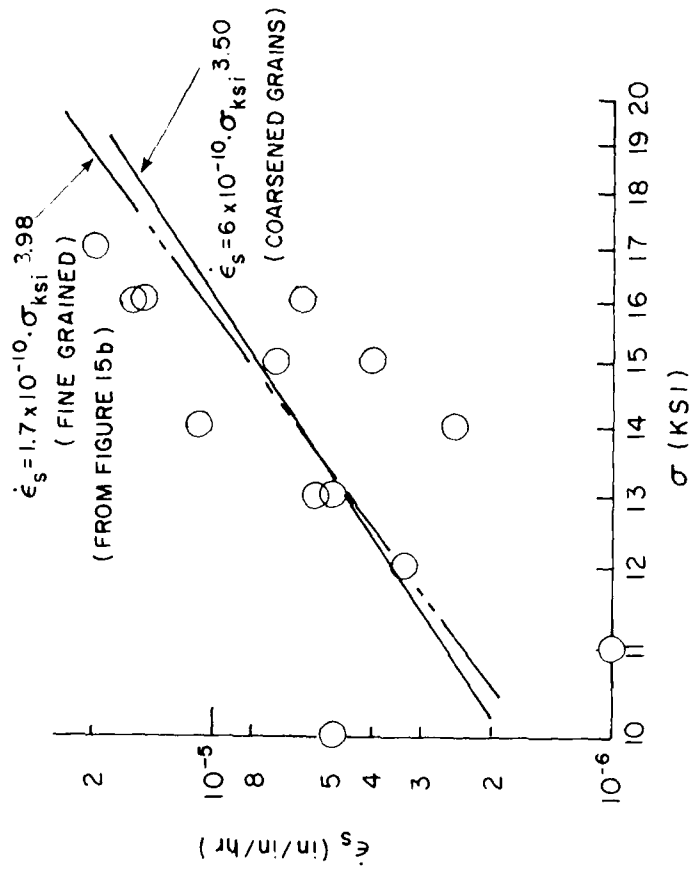


FIGURE 17 - EFFECT OF COARSENEED GRAINS ON THE 450°F CREEP PROPERTIES OF Al - 4Ti.

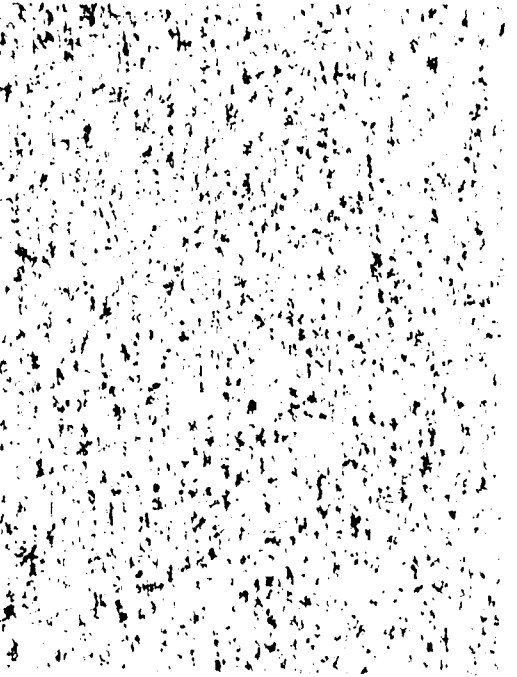
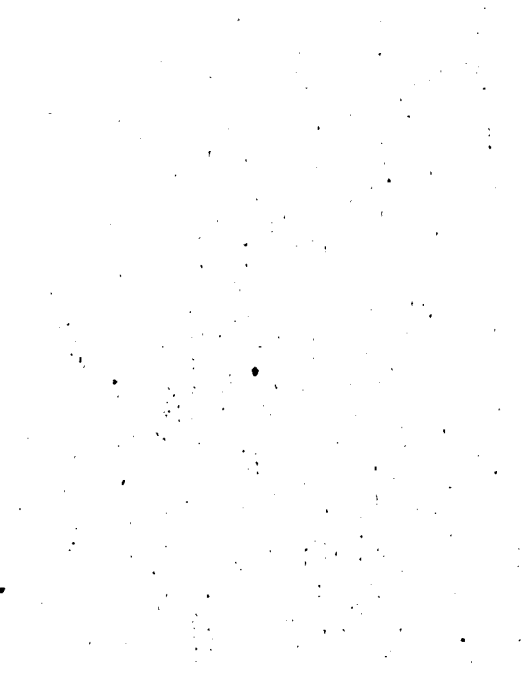
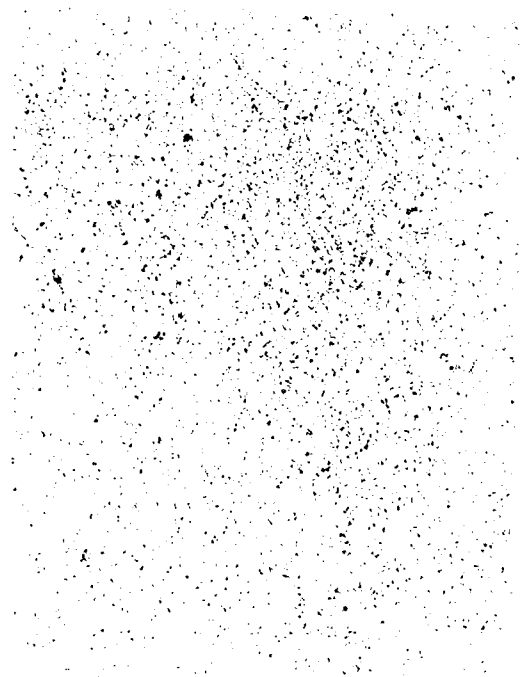


(a) PRIMARY CREEP STRAIN



(b) STEADY-STATE CREEP RATE

FIGURE 18 - EFFECT OF COARSENEED GRAINS ON THE 650°F CREEP PROPERTIES OF Al-4 Ti.



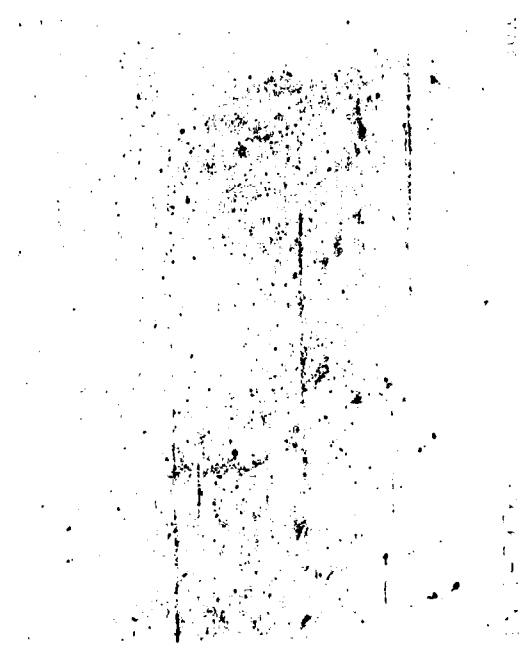
100-1000000

100-1000000

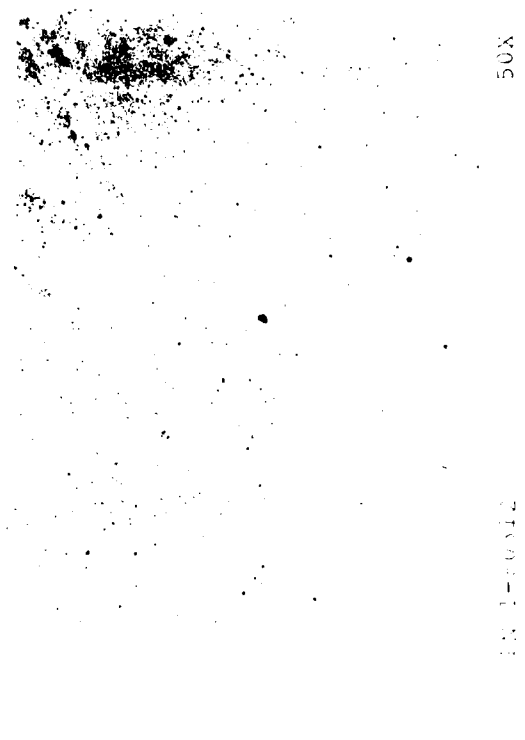
100-1000000

LONGITUDINAL SECTION

TRANSVERSE SECTION



50X

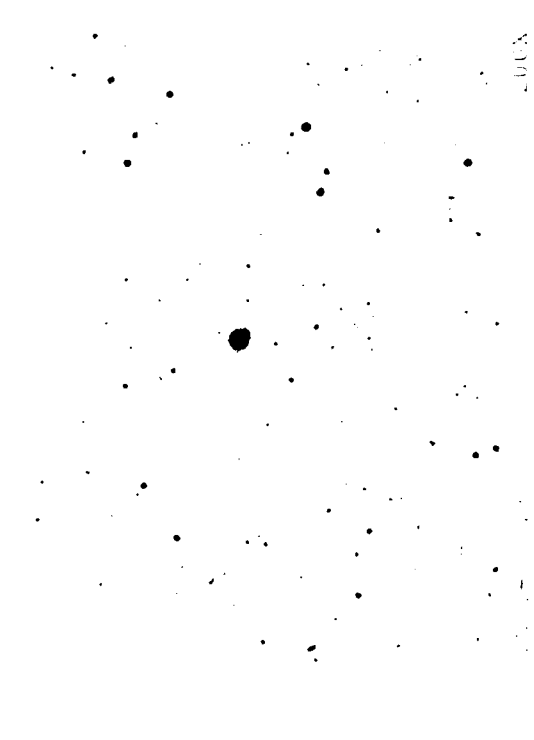


50X

IN 1-10012



200X



200X

Figure 11: Microstructure of W A Al-6.63n.



TEM 021141 63,000X



TEM 021696 63,000X



TEM 021142 63,000X



TEM 021697 63,000X

These four micrographs show the same field of view as the four micrographs on the previous page, but with different contrast settings.

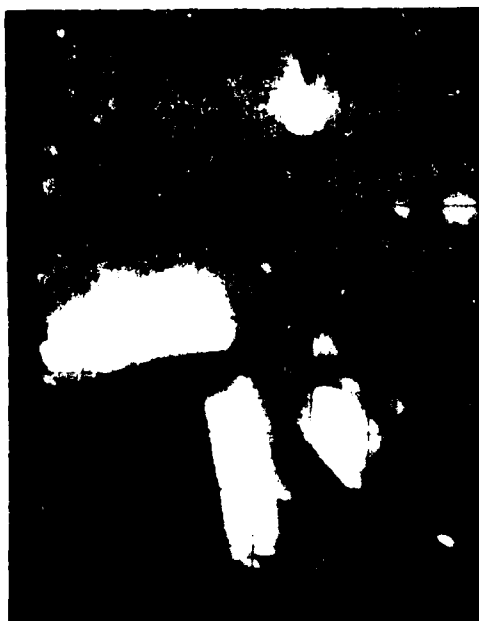
This image shows a blank white page with several small, dark specks scattered across it, which appear to be scanning artifacts or dust particles. There is no text or other graphical content.

This image shows a blank white page. There are several small, dark specks scattered across the surface, which appear to be scanning artifacts or dust particles. No text, figures, or tables are present.

[illegible]



4938-1-74



11th. Valley Section

50X

EX 1-60471

50X

EX 1-60471

EX 1-60471

EX 1-60471

Longitudinal Section

Transverse Section

IN 1-80300

50X

PL 1-80583

50X



63,000X



63,000X



63,000X

Electron Micrograph of a Cell - 63,000X, Al-1, Tm-1 and Tm-2

Microstructure of N/A Al-1.6Ni

Microstructure of N/A Al-1.6Ni



Figure 1.4: Microstructure of N/A Al-1.6Ni.

Longitudinal Section

Transverse Section

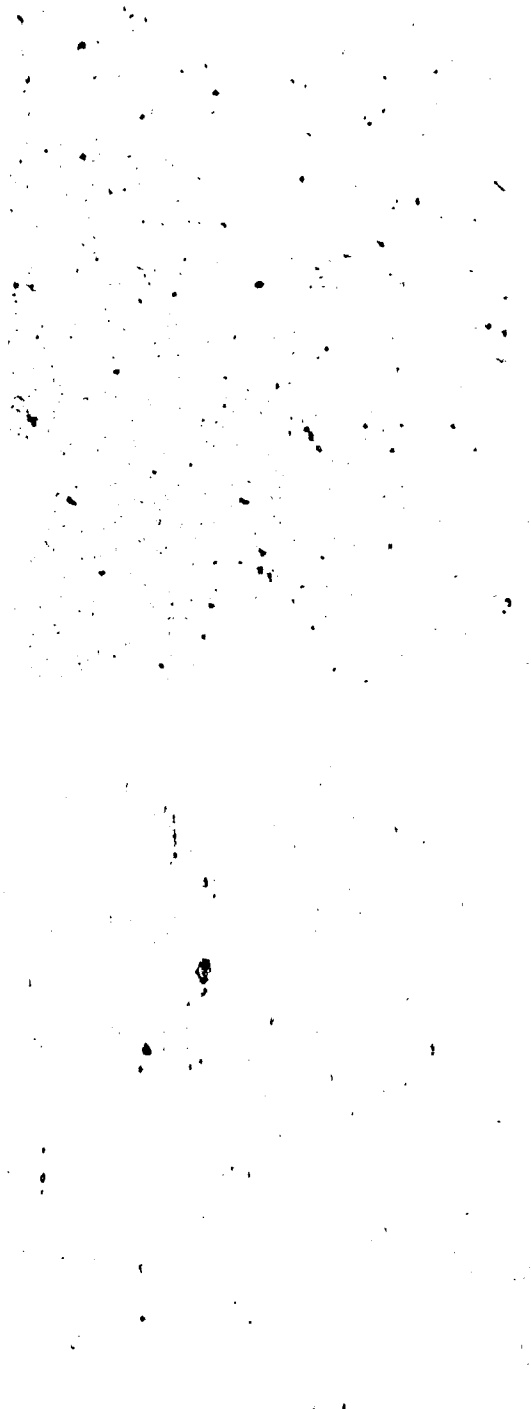


PN 1-77644

50X

PN 1-77644

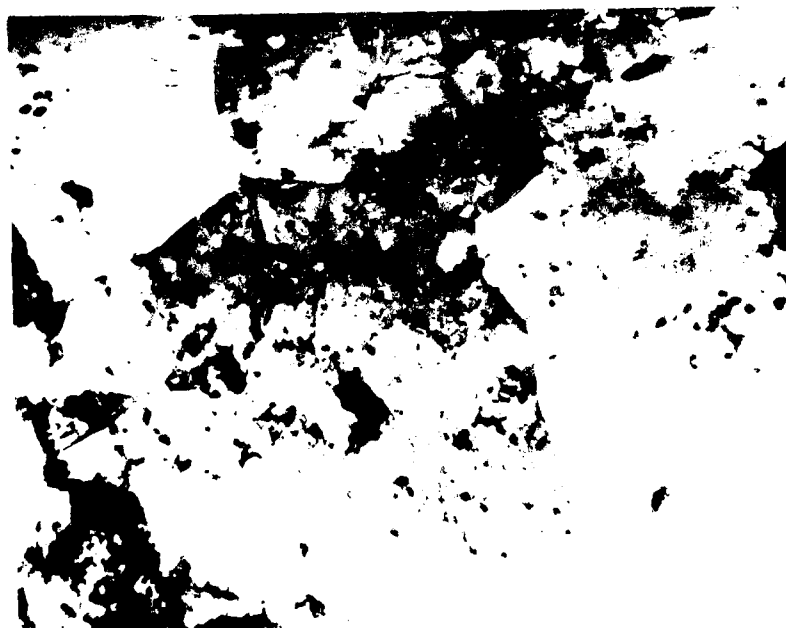
50X



Microstructure of M2 Al-1.1%

TEM 021190

FIRE DEPT. 10110



TEM 021193

FIRE DEPT. 10110

FIGURE 1. THE ABOVE PHOTOGRAPH IS A CLOSE-UP OF THE
FIRE DEPT. 10110



TEM 021186

63,000X

(a)

Al-1.6Ni

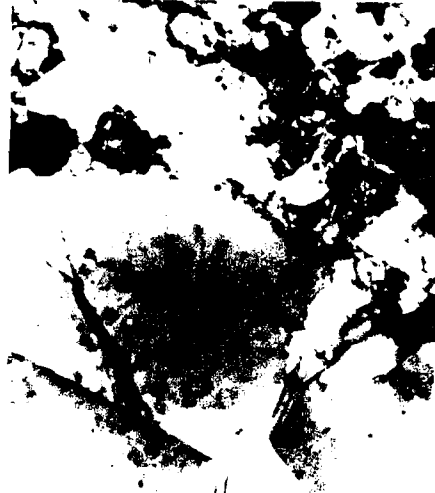


TEM 021196

63,000X

(b)

Unincorporated Ni

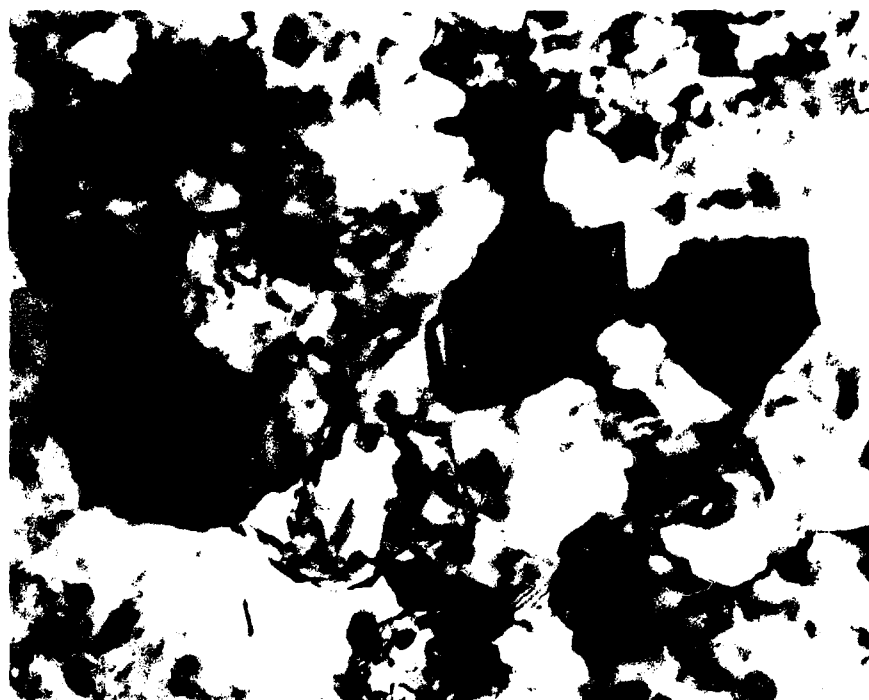


TEM 021197

63,000X

Unincorporated Ni

Unincorporated Ni



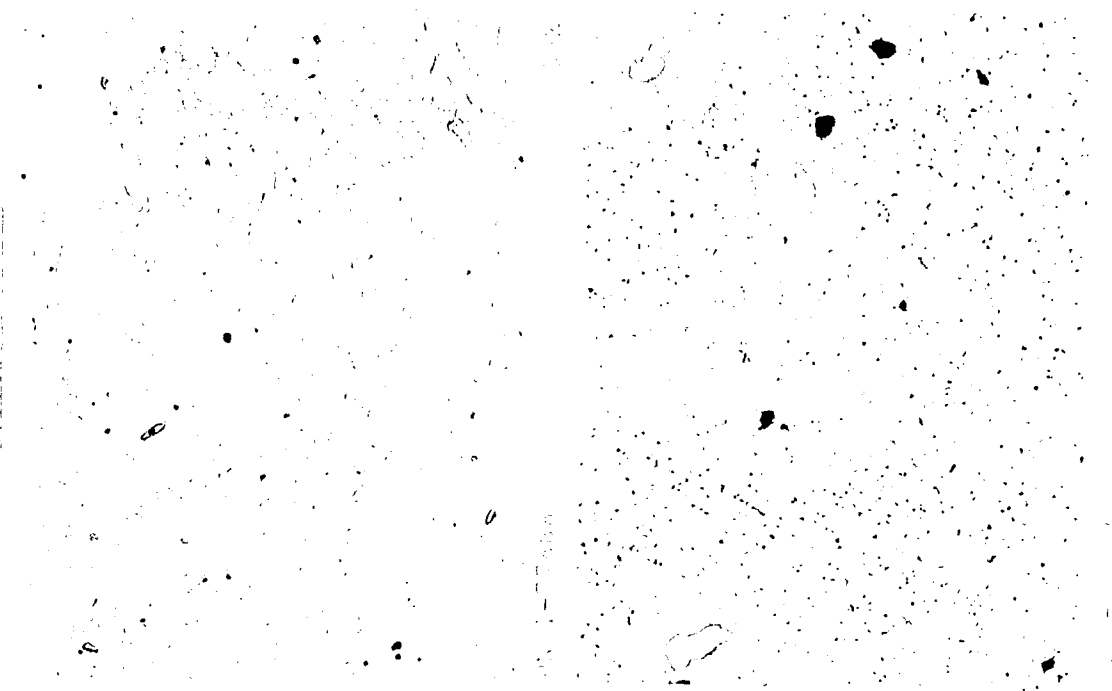
TEM 021208

63,000X

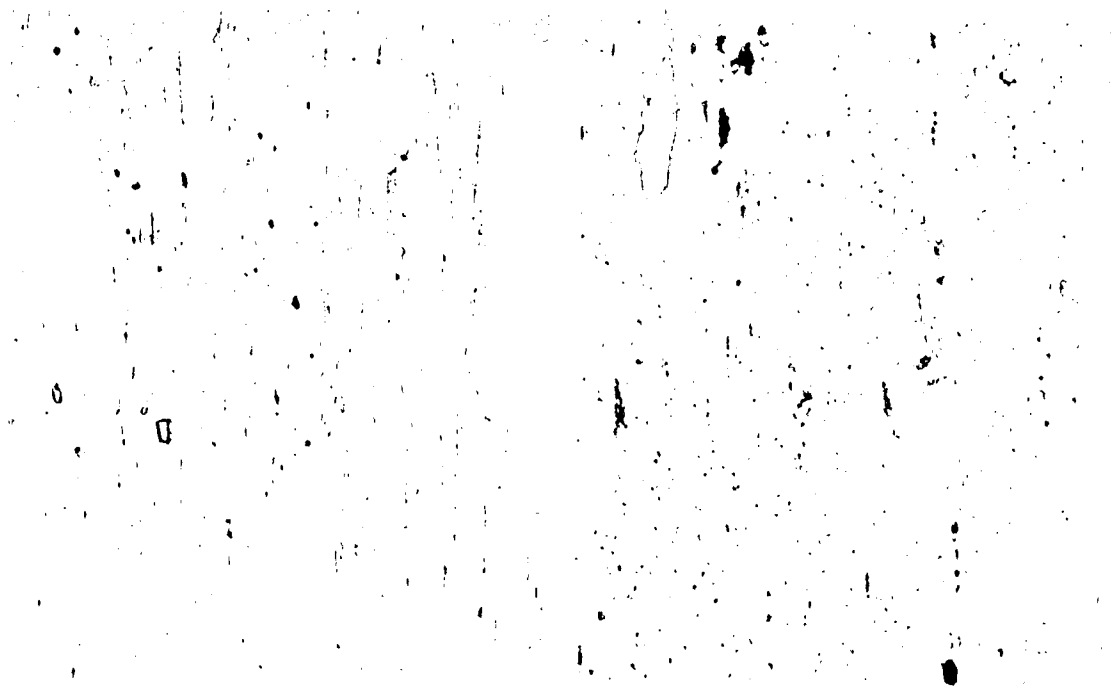
(f)
Al-1.1Fe

FIGURE 33: No evidence of grain coarsening in M/A Al-1.1Fe alloy.

Transverse section



Longitudinal section



Longitudinal section

Transverse section

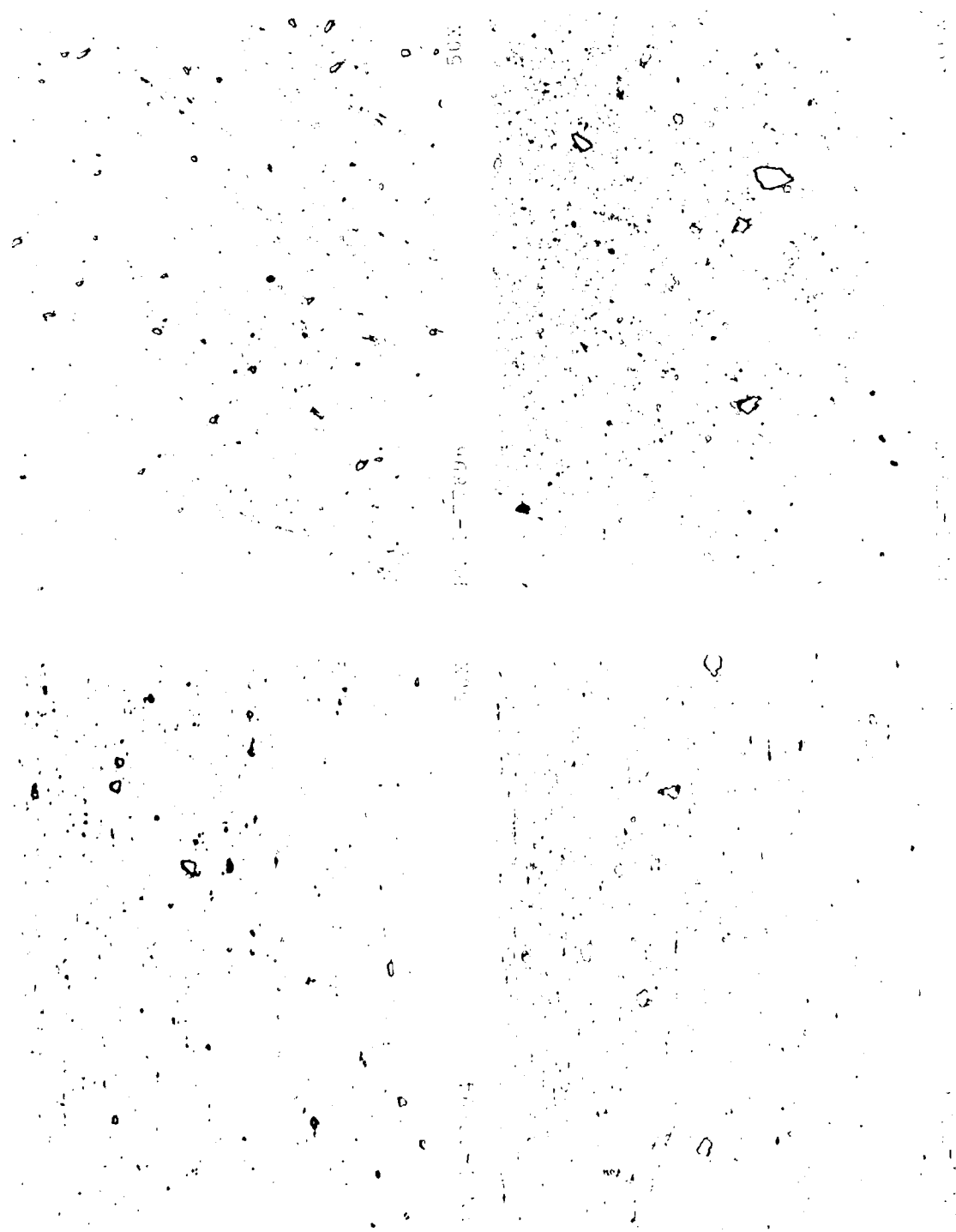
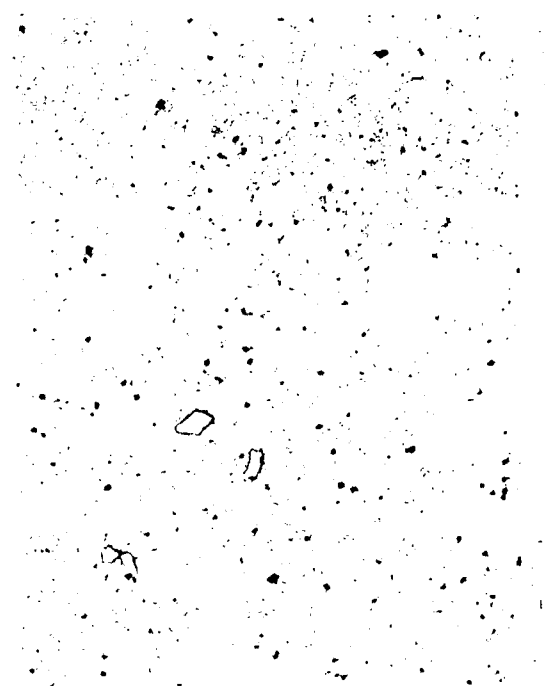
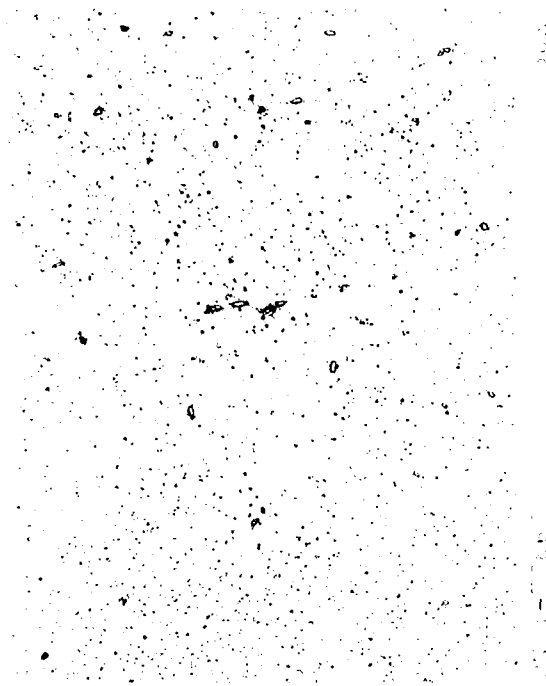
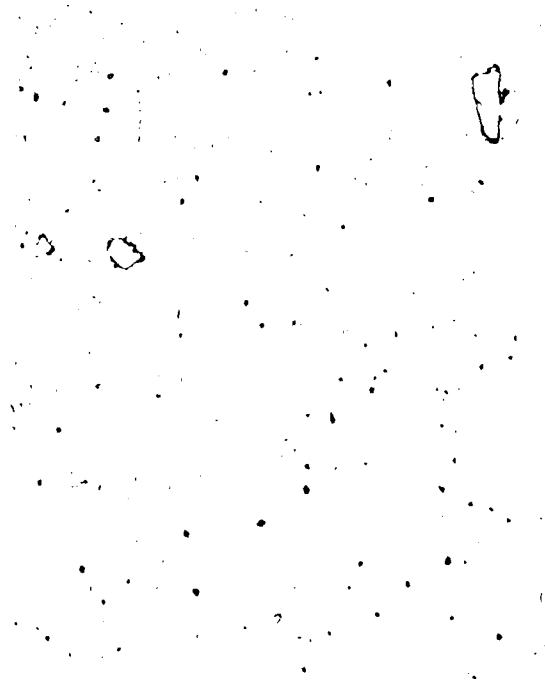
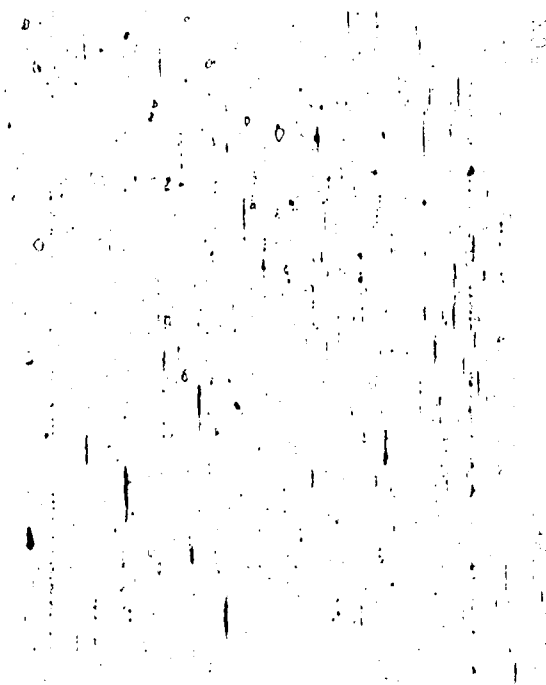


FIGURE 35: Microstructure of W-A1-1.6Fe-1.7Cr.

Transverse Section



Longitudinal Section



Longitudinal section



IN 1-79060

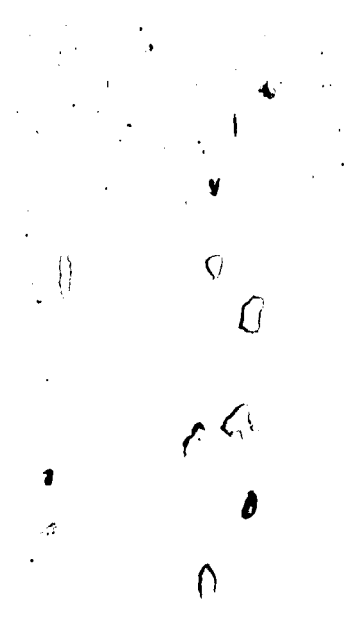
50X

Transverse section



IN 1-79382

50X



IN 1-79060

50X

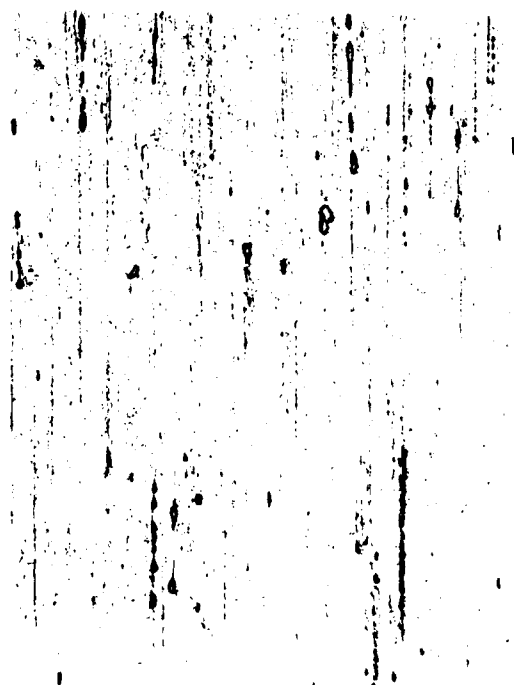


IN 1-79382

50X

FIGURE 7: Microstructure of V A Al-1.6 Ti-1.4 Ti.

Longitudinal Section



PA 1-77864

50X

Transverse Section



PA 1-77864

50X

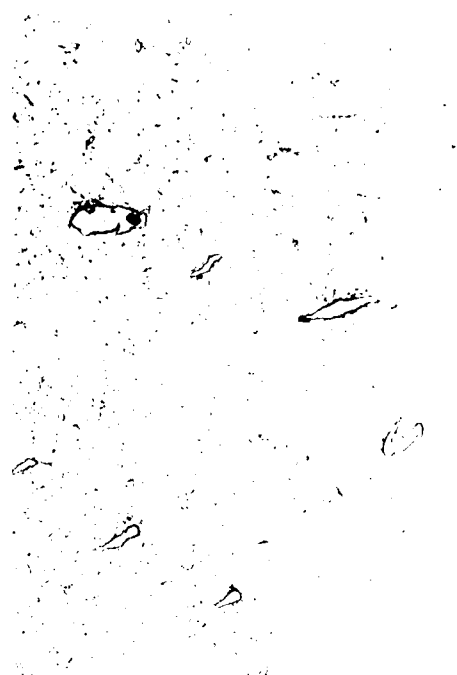
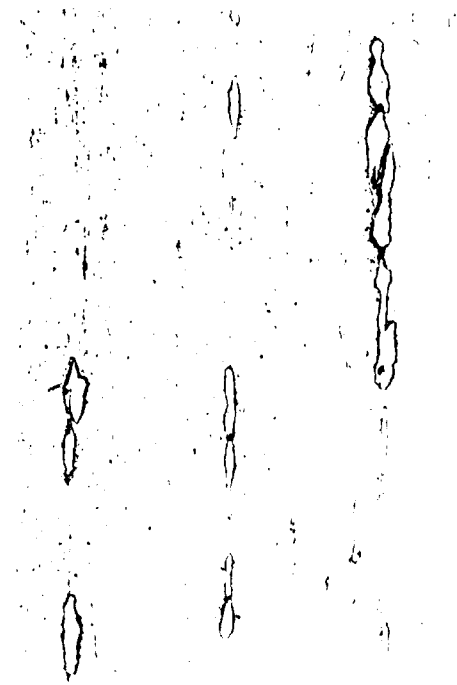


FIGURE 1. MICROSTRUCTURE OF V-Al-Ti.

DATE
FILMED

480